

NIST Measurement Services:

NIST Pressure Calibration Service

**NIST
Special
Publication
250-39**

Vern E. Bean

**U.S. Department of Commerce
Technology Administration**
National Institute of Standards and Technology

NIST MEASUREMENT SERVICES:

NIST Pressure Calibration Service

Vern E. Bean

Chemical Science and Technology Laboratory
National Institute of Standards and Technology
Gaithersburg, MD 20899

February 1994



U.S. Department of Commerce
Ronald H. Brown, Secretary

Technology Administration
Mary L. Good, Under Secretary for Technology

National Institute of Standards and Technology
Arati Prabhakar, Director

National Institute of Standards and Technology Special Publication 250-39
Natl. Inst. Stand. Technol. Spec. Publ. 250-39, 98 pages (Feb. 1994)
CODEN: NSPUE2

U.S. GOVERNMENT PRINTING OFFICE
WASHINGTON: 1994

For sale by the Superintendent of Documents, U.S. Government Printing Office, Washington, DC 20402-9325

PREFACE

This document describes the NIST Pressure Calibration Service so that others may benefit from the years of experience of the NIST pressure metrologists. It is snapshot of the service on 1 October 1992. Since pressure metrology is an active area of research at NIST, this document will become dated as methods, apparatus and uncertainties improve.

TABLE OF CONTENTS

	page
I. NIST PRESSURE CALIBRATION SERVICE.	1
II. DESIGN PHILOSOPHY AND THEORY.	1
A. Mercury Manometer.	1
B. Controlled-clearance Primary Standard Piston Gages.	4
1. Mass.	7
2. Local acceleration due to gravity.	7
3. Air buoyancy correction.	8
4. Surface tension correction.	9
5. Dimensional metrology of the piston.	11
6. Temperature correction.	13
7. Piston distortion.	14
8. Cylinder distortion.	15
9. Jacket pressure.	19
C. Total Uncertainty of the Primary Standards.	22
D. Transfer Standards and Their Uncertainty.	31
E. Calibration Quality Control.	36
III. CROSS-FLOAT CALIBRATION TECHNIQUE.	42
A. Experimental Arrangement.	43
B. Reference Levels.	47
C. Connections.	49
D. Cleaning.	50
E. Rotation.	51
F. Data Evaluation.	51
IV. INTERNATIONAL INTERCOMPARISONS.	53
A. IMGC.	53
B. BIPM.	58
V. REFERENCES.	63
VI. APPENDIX: SAMPLE CALIBRATION REPORT.	65

I. NIST PRESSURE CALIBRATION SERVICE

The National Institute of Standards and Technology (NIST) provides calibration services for piston gages and pressure transducers. For gas-operated units, the current pressure range is 7 kPa to 17 MPa (1 to 2500 psi); for oil, the range is 1.1 to 280 MPa (160 to 40,000 psi). Special tests for gas-operated units may be performed as low as 1.4 kPa. Routine calibrations of piston gages are done using the cross-floating technique with NIST transfer standard piston gages. The uncertainties in piston gage effective areas associated with the NIST transfer standard piston gages are plotted in figures 1 and 2 as a function of pressure for gas and oil respectively. Both plots represent the use of several transfer standards. For gas, the uncertainty ranges between 22 to 50 parts per million (ppm); for oil, it ranges between 40 and 86 ppm. The uncertainties are based on tripled standard deviations and are discussed in Sections II.C and II.D.

Shipping instructions and scheduling are available by telephoning the Pressure Group at (301) 975-4832 for gas-operated gages or (301) 975-4857 for oil-operated gages. The Group Secretary can be reached at (301) 975-4840.

II. DESIGN PHILOSOPHY AND THEORY

A primary standard for pressure is an instrument that does not require a pressure calibration in order to measure pressure; it is characterized by measuring the fundamental units of mass, time, length and temperature. Primary standards are used to calibrate NIST transfer standard piston gages, which are then used to calibrate customers' gages. The primary standards to which the NIST transfer standards are traceable are a mercury manometer and controlled-clearance piston gages.

In this section we consider design and operation of the primary standards, estimated uncertainties for the NIST primary standards, characterization of the NIST transfer gages, and the errors due to the calibration process of the transfer gages.

A. Mercury Manometer

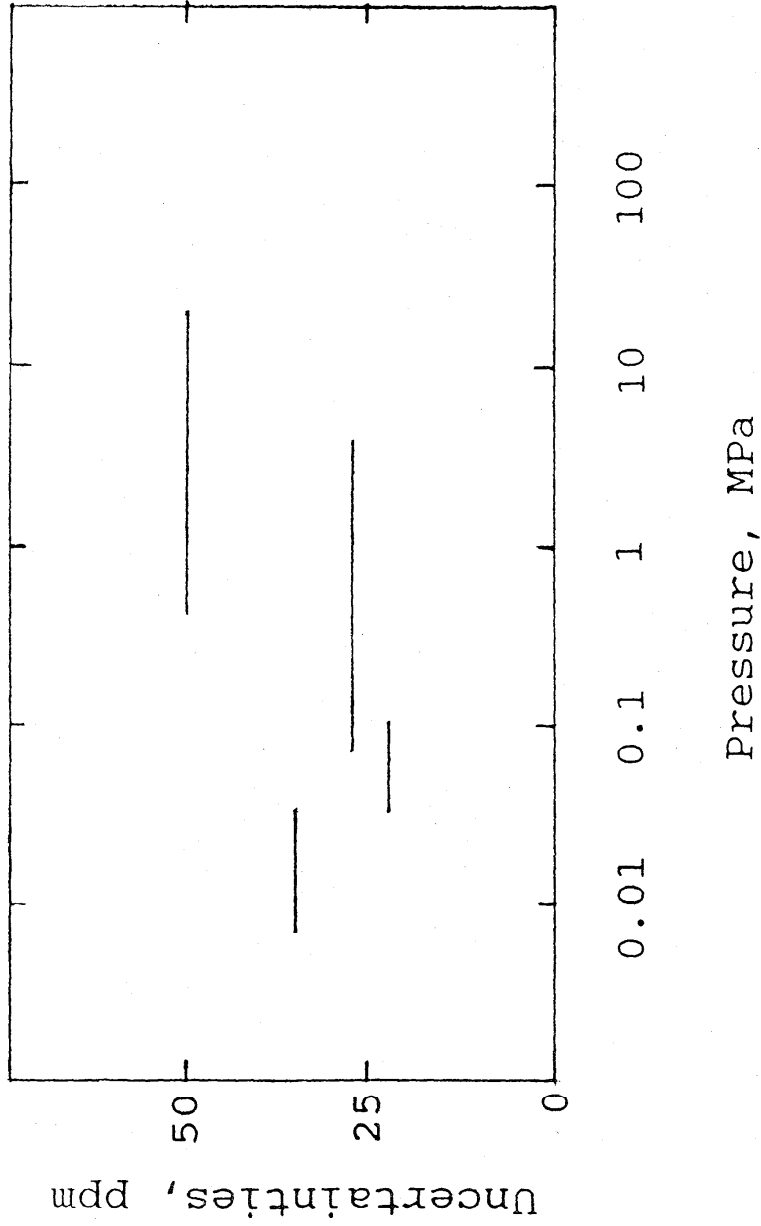


Figure 1. Uncertainties of the effective areas of the NIST gas-operated pressure transfer standards for nitrogen in the gage mode plotted as a function of pressure.

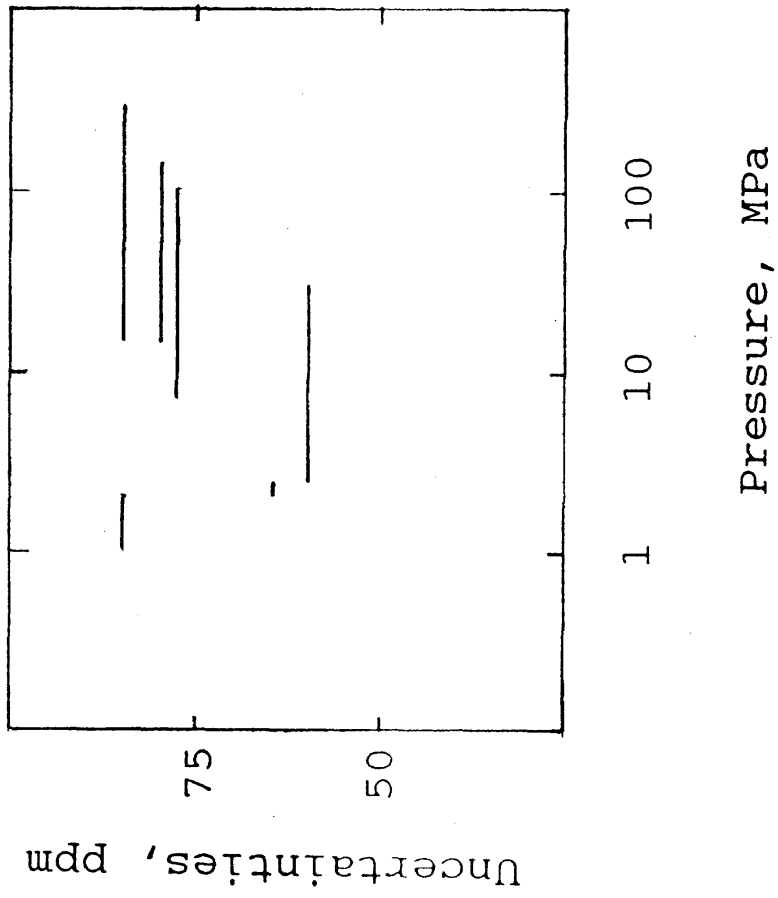


Figure 2. Uncertainties of the effective areas of the NIST oil-operated pressure transfer standards plotted as a function of pressure.

The essential feature of a manometer is a vertical column of fluid, suitably contained and supported at the bottom by an applied pressure. The magnitude of the pressure is the product of the column height, the density of the fluid, and the acceleration due to gravity plus whatever pressure is applied to the top surface of the fluid column. Thus the manometer is a differential pressure measurement device and is used in the absolute mode when the space above the top surface of the fluid column is evacuated, or in the gage mode when that space is at ambient atmospheric pressure. The greatest limitations of accuracy are due to the uncertainties in the density of the fluid and in the column height measurements. In general, at atmospheric pressure, a state-of-the-art manometer will have a lower uncertainty than a state-of-the-art primary standard piston gage.

The piston gage has two advantages over the manometer: portability and ease of use. These two properties and the stability of the piston gage make it an excellent transfer standard. In order to meet the demand for reduced uncertainties, we have used the manometer that was developed at the National Bureau of Standards (now NIST) for gas thermometry [1] as a primary standard to calibrate two essentially identical piston gages, designated as PG28 and PG29, that serve as the reference standards for the NIST gas pressure calibration service. PG28 then was used to calibrate several of the transfer standards used routinely in the calibration service.

A complete description of the gas thermometer manometer and an evaluation of its uncertainties are found in the literature [1-4]. The manometer operates at pressures up to 0.13 MPa in the absolute mode with an uncertainty of 2 ppm based on tripled standard deviations.

B. Controlled-Clearance Primary Standard Piston Gages

The controlled-clearance piston gage has been described by Heydemann and Welch [5] from which portions of the present discussion have been extracted.

Essentially, a piston gage is a piston fitted into a matching

cylinder filled with fluid, loaded with known weights, and rotated with respect to the cylinder to help attain concentricity of the piston in the cylinder. The rotation both minimizes the possibility of and aids in the detection of metal-to-metal contact, which causes unwanted frictional forces. The upward force due to the pressure in the system acting on the area of the piston is balanced against the downward gravitational force due to the weights. The pressure is defined as the ratio of the downward force to the area.

As the force can be measured with greater accuracy than the area, the limitation of the accuracy of the gage is in the determination of the area and how it changes with pressure due to elastic distortion of the piston and cylinder.

One method of reducing the effect of the distortion is to provide a means of applying an auxiliary pressure (known as the jacket pressure) to the outer surface of the cylinder to control the width of the annulus between the piston and the cylinder, as in the controlled-clearance piston gage shown in figure 3.

As the effect on the area due to the elastic distortion of the cylinder is several times that due to the piston, controlling the distortion of the cylinder can provide a significant reduction of inaccuracy. Furthermore, the ability to control the clearance allows one to obtain the best operating conditions for the particular pressure transmitting fluid used.

The pressure, p , generated by a controlled-clearance piston gage operating at its reference level is given by

$$P = \frac{Mg(1 - \rho_a/\rho_m) + \gamma C}{A_0 [1 + (\alpha_c + \alpha_p)(T - T_r)] (1 + bp_n) [1 + d(p_z - p_j)]} \quad (1)$$

where:

M is the mass of the piston plus the total load applied to the piston,

g is the local acceleration due to gravity,

ρ_a is the density of the air,

ρ_m is the density of the metal from which the weights are made,

γ is the surface tension of the fluid,

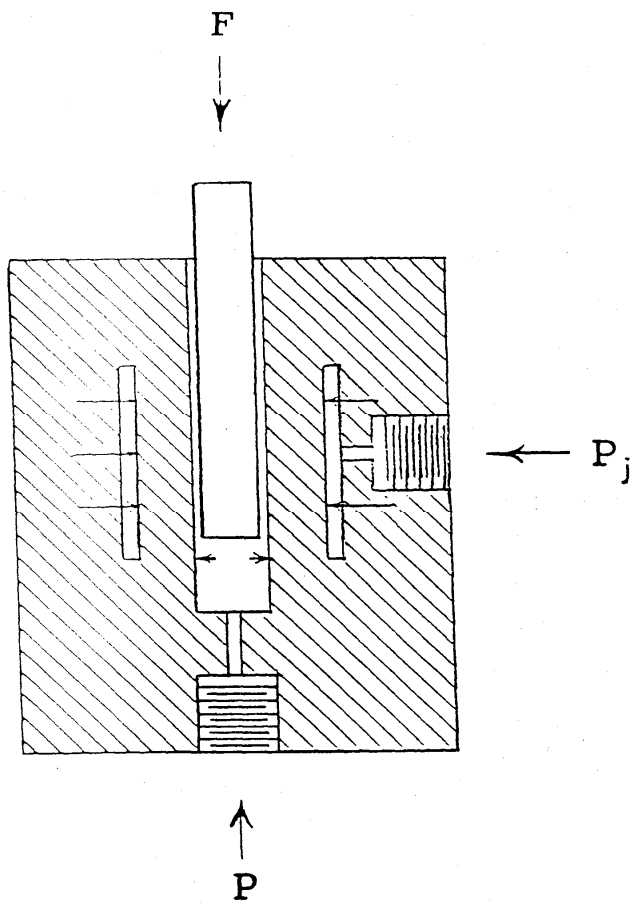


Figure 3. Schematic representation of a controlled-clearance piston gage where P is the pressure under the piston, F is the total force applied to the piston, and p_j is the jacket pressure.

C is the circumference of the piston where it emerges from the fluid,

A_0 is the area of the piston at the reference temperature T_r and at atmospheric pressure,

α_c is the linear thermal expansion coefficient for the cylinder,

α_p is the linear thermal expansion coefficient for the piston,

T is the temperature of the piston and cylinder at the time of the pressure measurement,

b is the pressure coefficient of the piston,

p_n is the nominal pressure,

d is the coefficient of the change of area with jacket pressure,

p_j is the jacket pressure during operation, and

p_z is the jacket pressure for which the clearance between the piston and cylinder is extrapolated to go to zero.

As all of the terms in eq (1) must be determined, we shall consider each in turn.

1. Mass

The values of the masses of all the weights used in the NIST pressure calibration service are traceable to the NIST Mass Standards Laboratory. An identifying number stamped into each weight is used to recall the appropriate mass value and density from computer memory. Mass values must be known for all parts of the piston gage supported by the pressure including the piston, weight hanger or yoke, the weights, and may include thrust bearings, rotation mechanisms, etc.

2. Local acceleration due to gravity.

The best value of g for a given laboratory site may be obtained by having on-site measurements made by the Office of National Geodetic Survey, with uncertainties on the order of 0.1 ppm or better. The next best value of g can be obtained by an interpolation from a grid of measurements prepared by the same organization, with typical uncertainties of a few ppm depending on geographical location. For further information on both of these services, contact National Oceanic and Atmospheric Administration,

National Ocean Survey, Office of the National Geodetic Survey, Geodetic Information Center, Washington Science Center, Rockville, MD 20852, [(301) 713-3242].

As a third option, the local acceleration due to gravity, g can be computed from

$$g = g_{\phi} - 0.0003086h + 0.0001118(h - h^1) \quad (2)$$

where g_{ϕ} is the sea level acceleration due to gravity, h is the elevation in meters of the site above sea-level, and h^1 is the elevation in meters of the general terrain for a radius of 70 km. g_{ϕ} is calculated from

$$g_{\phi} = 980.6160(1 - 0.0026373 \cos 2\phi + 0.0000059 \cos^2 2\phi) \quad (3)$$

where ϕ is the latitude. The value of g calculated in this manner may have an uncertainty of between 10 and 100 ppm depending on the locality. Without going to geographic extremes, g can vary by 0.1% within the continental United States.

The value of g we used until recently was measured in Room 129 of the Mechanical Engineering Building, NIST, Gaithersburg, and is $9.801018 \pm 0.000005 \text{ m s}^{-2}$ [6]. The value of g used since 1983, measured in Room A46 of the Metrology Building, is $9.801011 \pm 0.000002 \text{ m s}^{-2}$.

3. Air buoyancy correction.

The air buoyancy correction is given by $1 - \rho_a / \rho_m$ and is quite large. For example, it is 147.5 ppm at 23 °C, 30 percent relative humidity, and 100 kPa barometric pressure for a stainless steel weight of density 8 g/cm^3 . The density of moist air has been tabulated [7,8]. It can be computed from [9]

$$\rho_a = \frac{0.0034836 (P - 0.0037960 U e_s)}{TZ} \quad (4)$$

where P is the barometric pressure in Pa, U is the percent of

relative humidity, e_s is the saturation vapor pressure of water, T is the air temperature in kelvins, Z is the compressibility factor for moist air. ρ_a is expressed in kg m^{-3} . The appropriate values of e_s can be calculated from

$$e_s = 1.7526 \times 10^{11} e^{\frac{-5315.56}{T}} \quad (5)$$

where e is the base of natural logarithms. Values of Z are listed in table 1.

A piston gage is a differential pressure measurement device measuring the difference of the pressures applied to the top and bottom of the piston. When the gage is used with the top of the piston at ambient atmospheric pressure, the unit is operating in the gage mode. When the gage is used with the top of the piston in a vacuum, the unit is operating in the absolute mode. When the piston gage is used in the gage mode, the values for the densities of the metals from which the weights are made and which are used in the calculation of the air buoyancy correction must be the identical values used by the mass laboratory when the true mass values are calculated. For this case, the density values can be arbitrary in the sense that they need not be correct for the metal in question, but they must be identical to the values used by the mass laboratory.

The situation is different for the absolute mode. Since in the absolute mode, the air buoyancy force is reduced to zero by evacuating the space around the weights, an incorrect mass density value used by the mass laboratory will result in an error in the mass value. An error of 1 percent in the metal density yields an error of 1.5 ppm in the pressure. In this case it may be necessary to determine the density values of the weights by hydrostatic weighing.

All of the NIST controlled-clearance piston gages operate only in the gage mode.

4. Surface tension correction.

Table 1. Compressibility factor, Z, for CO₂-free air

Temperature (Celsius)	Pressure		Relative Humidity in Percent				
	(pascals)	(mm Hg)	0	25	50	75	100
19.0	70000	525.0	.99973	.99972	.99971	.99968	.99966
	75000	562.5	.99972	.99970	.99969	.99967	.99964
	80000	600.0	.99970	.99968	.99967	.99965	.99963
	85000	637.6	.99968	.99967	.99965	.99963	.99961
	90000	675.1	.99966	.99965	.99963	.99961	.99959
	95000	712.6	.99964	.99963	.99961	.99960	.99957
	100000	750.1	.99962	.99961	.99959	.99958	.99956
	101325	760.0	.99962	.99960	.99959	.99957	.99955
	105000	787.6	.99960	.99959	.99958	.99956	.99954
	110000	825.1	.99958	.99957	.99956	.99954	.99952
20.0	70000	525.0	.99974	.99973	.99971	.99969	.99966
	75000	562.5	.99972	.99971	.99969	.99967	.99964
	80000	600.0	.99970	.99969	.99967	.99965	.99963
	85000	637.6	.99969	.99967	.99966	.99964	.99961
	90000	675.1	.99967	.99966	.99964	.99962	.99960
	95000	712.6	.99965	.99964	.99962	.99960	.99958
	100000	750.1	.99963	.99962	.99960	.99958	.99956
	101325	760.0	.99963	.99961	.99960	.99958	.99956
	105000	787.6	.99961	.99960	.99958	.99957	.99954
	110000	825.1	.99959	.99958	.99957	.99955	.99953
21.0	70000	525.0	.99975	.99973	.99971	.99969	.99966
	75000	562.5	.99973	.99972	.99970	.99967	.99964
	80000	600.0	.99971	.99970	.99968	.99966	.99963
	85000	637.6	.99969	.99968	.99966	.99964	.99961
	90000	675.1	.99968	.99966	.99965	.99962	.99960
	95000	712.6	.99966	.99965	.99963	.99961	.99958
	100000	750.1	.99964	.99963	.99961	.99959	.99956
	101325	760.0	.99964	.99962	.99961	.99959	.99956
	105000	787.6	.99962	.99961	.99959	.99957	.99955
	110000	825.1	.99960	.99959	.99958	.99956	.99953
23.0	70000	525.0	.99976	.99975	.99972	.99969	.99966
	75000	562.5	.99974	.99972	.99970	.99968	.99964
	80000	600.0	.99973	.99971	.99969	.99966	.99963
	85000	637.6	.99971	.99969	.99967	.99965	.99962
	90000	675.1	.99969	.99968	.99966	.99963	.99960
	95000	712.6	.99968	.99966	.99964	.99962	.99959
	100000	750.1	.99966	.99964	.99962	.99960	.99957
	101325	760.0	.99965	.99964	.99962	.99960	.99957
	105000	787.6	.99964	.99963	.99961	.99958	.99956
	110000	825.1	.99963	.99961	.99959	.99957	.99954
24.0	70000	525.0	.99977	.99975	.99973	.99969	.99965
	75000	562.5	.99975	.99973	.99971	.99968	.99964
	80000	600.0	.99973	.99972	.99970	.99967	.99963
	85000	637.6	.99972	.99970	.99968	.99965	.99962
	90000	675.1	.99970	.99969	.99966	.99964	.99960
	95000	712.6	.99968	.99967	.99965	.99962	.99959
	100000	750.1	.99967	.99965	.99963	.99961	.99957
	101325	760.0	.99966	.99965	.99963	.99960	.99957
	105000	787.6	.99965	.99964	.99962	.99959	.99956
	110000	825.1	.99964	.99962	.99960	.99957	.99954
25.0	70000	525.0	.99977	.99976	.99973	.99970	.99965
	75000	562.5	.99976	.99974	.99971	.99968	.99964
	80000	600.0	.99974	.99972	.99970	.99967	.99963
	85000	637.6	.99973	.99971	.99968	.99965	.99962
	90000	675.1	.99971	.99969	.99967	.99964	.99960
	95000	712.6	.99969	.99968	.99965	.99962	.99959
	100000	750.1	.99968	.99966	.99964	.99961	.99958
	101325	760.0	.99967	.99966	.99963	.99961	.99957
	105000	787.6	.99966	.99964	.99962	.99960	.99956
	110000	825.1	.99965	.99963	.99961	.99958	.99955
26.0	70000	525.0	.99978	.99976	.99973	.99970	.99965
	75000	562.5	.99976	.99975	.99972	.99968	.99964
	80000	600.0	.99975	.99973	.99970	.99967	.99963
	85000	637.6	.99973	.99971	.99969	.99966	.99961
	90000	675.1	.99972	.99970	.99967	.99964	.99960
	95000	712.6	.99970	.99968	.99966	.99963	.99959
	100000	750.1	.99969	.99967	.99964	.99961	.99958
	101325	760.0	.99968	.99966	.99964	.99961	.99957
	105000	787.6	.99967	.99965	.99963	.99960	.99956
	110000	825.1	.99966	.99964	.99961	.99959	.99955

γC is the force generated by the surface tension of the fluid acting on the piston where it emerges from the fluid. γ is the surface tension of the fluid and C is the circumference of the piston where it emerges from the fluid. The value of the surface tension for the oil commonly used in NIST piston gages is 3.05×10^{-2} N/m and is assumed to be accurate within 10 percent. This is a small and perhaps negligible correction for high pressure gages but it may have to be taken into account for oil-operated gages at low pressures. For example, at 1.1 MPa, the correction for a gage with a piston diameter of 0.010 m is 11 ppm. This correction does not apply to gas-operated gages.

5. Dimensional metrology of the piston.

A_0 is the average cross-sectional area of the piston at atmospheric pressure as determined from numerous measurements of the diameter along the length of the piston. For a primary standard every effort is made to obtain a straight and round piston. Polar plots of the deviation of actual piston diameter from a nominal diameter are a useful way to check the roundness of the piston. Figure 4 is such a plot for the piston in the NIST controlled-clearance gage known as PG27 with a nominal diameter of 8 mm. In this case, the deviations from being perfectly round do not exceed 7.5 nm.

The Dimensional Metrology Group of NIST presently claims an uncertainty (one standard deviation) of 3.3×10^{-8} m in the determination of the diameter of pistons for primary gages irrespective of their diameter. Thus, on a part-per-million basis, a perfectly round and straight piston of large diameter will have a smaller uncertainty in area than a small diameter piston of equal quality.

The value of A_0 used in eq (1) is calculated using the expression

$$A_0 = \frac{1}{4} (\pi D^2) [1 + 2\alpha_p (23 - T_m)] \quad (6)$$

where D is the average piston diameter determined from the dimensional measurements and T_m is the temperature in °C at which

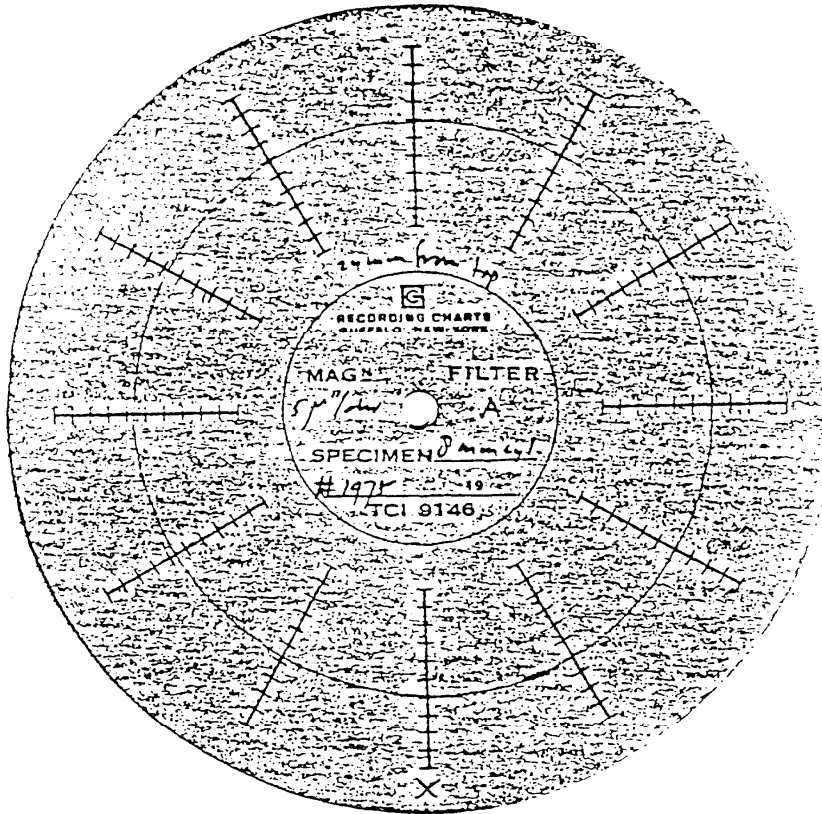


Figure 4. Talyron of the piston for PG27.

these measurements were made. This expression now defines T_r of eq (1) to be 23 °C. The NIST dimensional laboratory is maintained at 20 °C to match the dimensional laboratory temperatures of the European national standards laboratories while the NIST pressure laboratory is maintained at 23 °C to match the normal temperature of the pressure laboratories in American industry; hence, the temperature correction.

The appropriate value of D to use in eq (6) is a matter of judgment where one must consider the piston roundness, straightness, and the most probable location along its length where controlling the clearance between the piston and cylinder will define the gage's working area to be. The uncertainty assigned to the value of D must take into account all of these considerations as well as the uncertainties of the dimensional measurement process.

6. Temperature correction.

The temperature correction for the area is given by

$$C_T = 1 + (\alpha_c + \alpha_p) (T - T_r) \quad (7)$$

The reference temperature T_r is the temperature at which the piston area assumes the value A_0 . For a tungsten carbide piston inside a steel cylinder the correction is on the order of 17 ppm per °C.

An operating piston gage generates heat in three ways: (a) adiabatic heating in the fluid due to a rapid pressure change; (b) heat generated by friction in the fluid as it flows up the annulus; and (c) heat generated by the rotation of the piston.

The temperature gradient along the cylinder length of a hydraulic piston gage is due only to the heat generated by the flow of the fluid up through the annulus and is a function of pressure, viscosity and location along the engagement length. The only reported measurements of the temperature gradient are for a simple gage operating at 20 MPa. The maximum temperature difference between the fluid under the piston and the fluid at any location along the piston engagement length was of the order of 60 mK [10]. Heat generated by piston rotation and that due to adiabatic effects

serve only to increase the overall temperature of the system but do not contribute to the temperature gradient.

Temperature measurements of the cylinder of an operating gage as a function of jacket pressure indicate the temperature increases by several hundredths of a degree when a jacket pressure close to the upper end of the operating range is chosen. This rise has been used as an indication for the upper limit of the jacket pressure range.

Platinum resistance thermometers, thermocouples, and thermistors have been used to detect the small changes in temperature in piston gages.

The temperature sensing elements, leads, and read-out should be calibrated as a unit. The optimum location for the sensor would be at the working area of the piston and cylinder but this is seldom possible. Normally, the operating temperature of piston gages is determined either on the base supporting the cylinder or on the lower end of the cylinder, which is a compromise of the measurement. The effect of this compromise must be considered on a case-by-case basis because of the wide variety in gage design and in materials of construction.

Thermal expansivity data for many gage materials are listed in table 2.

7. Piston distortion.

The piston pressure coefficient, b , is computed from elastic theory using the expression [11]

$$b = \frac{(3\mu - 1)}{E} \quad (8)$$

where μ is Poisson's ratio and E is the modulus of elasticity for the material from which the piston is made. Both values can be obtained from ultrasonic measurements on the piston material with an uncertainty of less than 1 percent.

Pistons are frequently made from cemented tungsten carbide. Data for the elastic constants of this and other materials are listed in table 2. With the data for tungsten carbide C93, the piston distortion, bp_n , amounts to 2.3 ppm at 4 MPa and to 117 ppm at 200 MPa.

The calculation of the uncertainty for each parameter in eq (1) is discussed in Section C. The value of b is the only parameter of eq (1) that is determined from theory. Since no satisfactory way of determining the contribution to the uncertainty due to the inadequacy of the theory for calculating b is available, Heydemann and Welch [5] suggested that one might multiply the uncertainty for this term as determined in Section C by a factor of three as a conservative measure.

8. Cylinder distortion.

The cylinder distortion correction term is

$$C_d = 1 + d(p_z - p_j) \quad (9)$$

The value of d can be measured either of two ways:

1. Vary p_j and make corresponding changes in the load on the piston such that the generated pressure remains constant.
2. Measure the changes in the generated pressure corresponding to the changes in p_j .

Either method requires monitoring the generated pressure which can be done with any transducer of sufficient sensitivity and short term stability. In particular, it can be done with a second piston gage cross-floated against the controlled-clearance piston gage. In order to develop an expression to determine d from the first method, we rearrange eq (1) obtaining

$$W = pA_0 [1 + (\alpha_p + \alpha_c)(T - T_r)] (1 + b_p p) [1 + d(p_z - p_j)] \quad (10)$$

where W is the numerator of the right hand side of eq (1).

Let us designate the controlled-clearance gage as the standard

Table 2. Elastic constants, density and thermal expansivities of piston and cylinder materials

Material	Shear modulus G (N/m^2)	Young's modulus E (N/m^2)	Poisson's ratio μ	Thermal expansivity α (K^{-1})	Density ρ (g/cm^3)	Pressure coefficient (piston) β (m^2/N)
K9-steel	7.92×10^{11}	2.05×10^{11}	0.295			
'Hydurax' aluminum-bronze	5.36×10^{11}	1.43×10^{11}	0.333			
GEC heavy metal, tungsten alloy	14.2×10^{11}	3.67×10^{11}	0.286	5.8×10^{-6}	17	
Tungsten carbide K58*		6.11×10^{11}	0.209	4.54×10^{-6}	14.9	-6.10×10^{-13}
Tungsten carbide C93*		6.31×10^{11}	0.210	4.5×10^{-6}	15.1	-5.86×10^{-13}
Tungsten carbide K36		6.32×10^{11}	0.211	4.5×10^{-6}	14.9	-5.81×10^{-13}
Stainless steel AM-350 (precip. hardening)		2.03×10^{11}	0.300	11.4×10^{-6}	7.81	-4.93×10^{-13}
Erass	4.2×10^{10}	1.1×10^{11}		18	8.6×10^{-6}	

* Data from ultrasonic measurements.

and the other gage as the reference. The two piston gages are brought into balance with some given load on the reference gage. Then a series of small changes in p_j are made with corresponding changes in W on the standard such as to keep the two gages in balance. Experience has shown that during the time required for these measurements, the temperature change in both gages is of no consequence. Hence, as we apply eq (10) to the standard, the variables for the cross-float measurements are W , and p_j . In the term $1+bp_n$, bp_n is negligible compared to 1 for the present purpose and we will regard the entire term as invariant. Since d already has been used in eq (10), we use Δ to denote the total differential. The relative change in W for the standard gage becomes

$$\frac{\Delta W}{W} = \frac{d\Delta p_j}{1+d(p_z-p_j)} \quad (11)$$

For the purpose of determining d , we now assume $d(p_z-p_j)$ is negligible compared to 1. Solving for d , we obtain

$$d = - \frac{\Delta W}{W\Delta p_j} \quad (12)$$

For the second method where the change of the generated pressure is measured as a function of p_j , an analogous analysis yields

$$d = - \frac{\Delta p}{p\Delta p_j} \quad (13)$$

The value of d must be determined for a series of pressures over the operating range of the gage. The value of d is a function of the pressurizing fluid used in the gage and must be measured for each fluid.

Figure 5 is a plot of d as a function of load for PG27 which was determined by the cross-floating technique.

Experimental values of d are generally dependent upon the applied load. In order to have an expression for interpolation, we

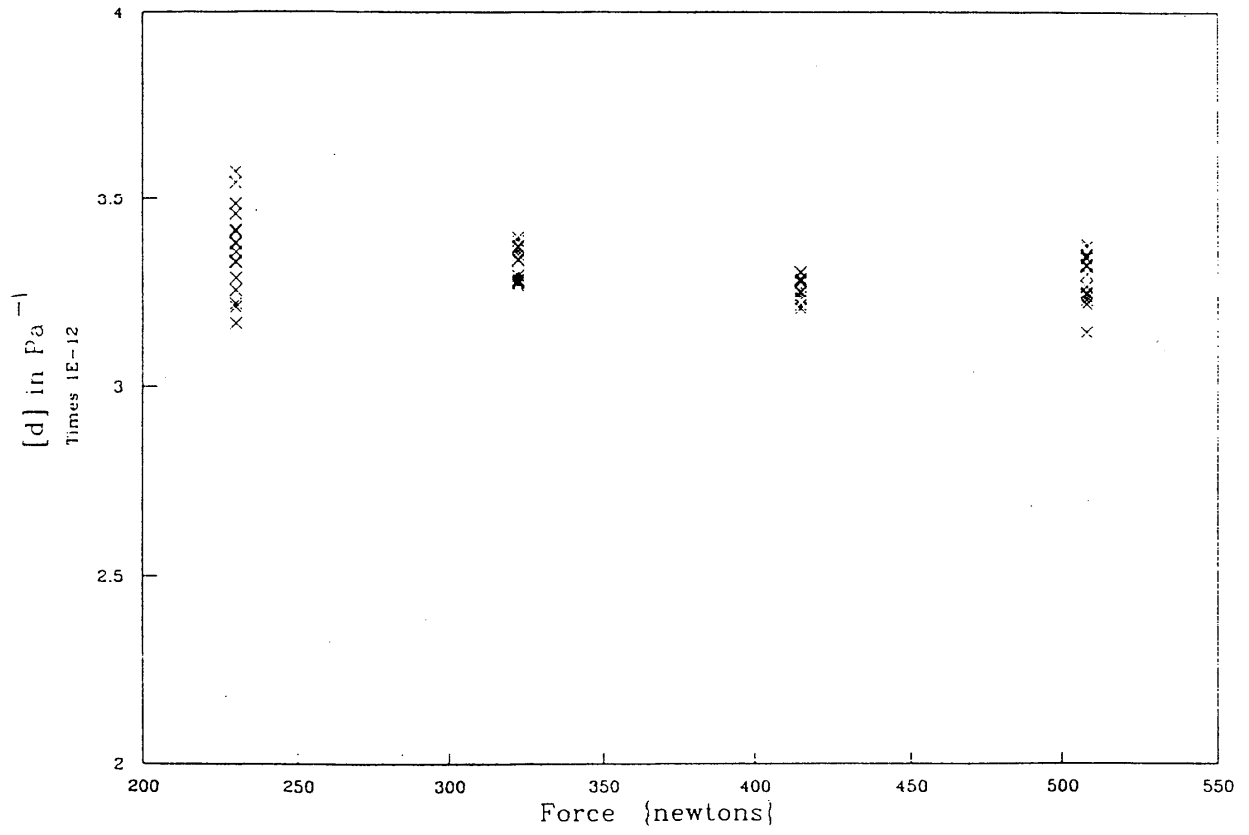


Figure 5. Experimental values of d plotted as a function of load.

find it convenient to use an empirical equation of the form

$$d = D + EW + FW^2 \quad (14)$$

which is fitted to the experimental values of d and W .

9. Jacket pressure.

To determine the jacket pressure for which the clearance c is reduced to zero we make the assumption that the leak rate past the piston is proportional to the third power of the clearance or that

$$(\partial V/\partial t)^{1/3} = \text{const} \cdot c \quad (15)$$

where V is the volume of oil bypassing the piston in time t . Equation (15) is the basic law for laminar flow between infinitely extended plane and parallel plates. Instead of observing the leak rate, $\partial V/\partial t$, it is equivalent and more convenient to measure the fall rate of the piston, $\partial s/\partial t$, where s is the vertical position of the piston. Now we rewrite eq (15) as

$$(\partial s/\partial t)^{1/3} = \text{const} \cdot c = \text{const} (p_z - p_j) \quad (16)$$

where we have assumed c is directly proportional to the difference between p_z and p_j . We can now determine p_z from a measurement of $\partial s/\partial t$ as a function of p_j .

The piston position of an operating piston gage can be conveniently measured with a non-contact capacitance proximity sensor. One method is to mount an aluminum disk on the top of the weight hanger directly over the piston and then position the sensor over the center of the disk. The output of the sensor is displayed on a 250 mm wide strip chart recorder. While the weight stack is resting on the bottom stops, we raise the disk with shims of known thickness and thereby calibrate the sensor-recorder combination. The sensor-recorder combination is adjusted such that the pen travels about 80 percent of its full range as the piston falls from 0.5 mm above its reference level to 0.5 mm below its reference level and the pen is at the center of the chart when the piston is

at its reference level. A stop watch is used to time the piston's fall through this central 1 mm. Abnormalities in the recorded trace are helpful in trouble-shooting.

Linear voltage displacement transducers, laser interferometers, and dial gages have also been used to make fall rate measurements.

The gage is valved off from the rest of the pressure system so as to be leak-tight with the exception of the leakage past the piston through the clearance. Fall rate measurements are then made as a function of jacket pressure for each of several different loads over the operating pressure range. During these measurements, the clearance must be large enough to maintain a fluid film between piston and cylinder at all times. The cube root of the fall rate is a linear function of the jacket pressure over part of the range. The data may deviate from this linear relationship at very high and very low jacket pressures. When either very high or very low jacket pressures are used the temperature of the piston and cylinder increases by several hundredths of a degree. At high values of p_j this is due to friction between piston and cylinder. At low jacket pressures it is due to viscosity in the oil passing through the clearance at high speed. Either region should be avoided. Friction between piston and cylinder may cause rapid deterioration of both.

In figure 6, the jacket pressure is plotted as a function of the cube root of the fall rate for several loads on PG27. The individual fall rate lines are extrapolated to zero fall rate where they intersect the vertical axis at corresponding values of p_z . The right hand side of figure 6 shows a plot of the p_z as a function of load. The extrapolation of this curve to zero load intersects the vertical axis at p_{z0} . A dashed line in the graph indicates the operating jacket pressures, which are chosen from the linear portions of the fall rate curves near the upper ends.

An equation of the form

$$p_j = p_z - K(\partial s / \partial t)^{1/3} \quad (17)$$

is fitted to data from within the linear portions of the curves of

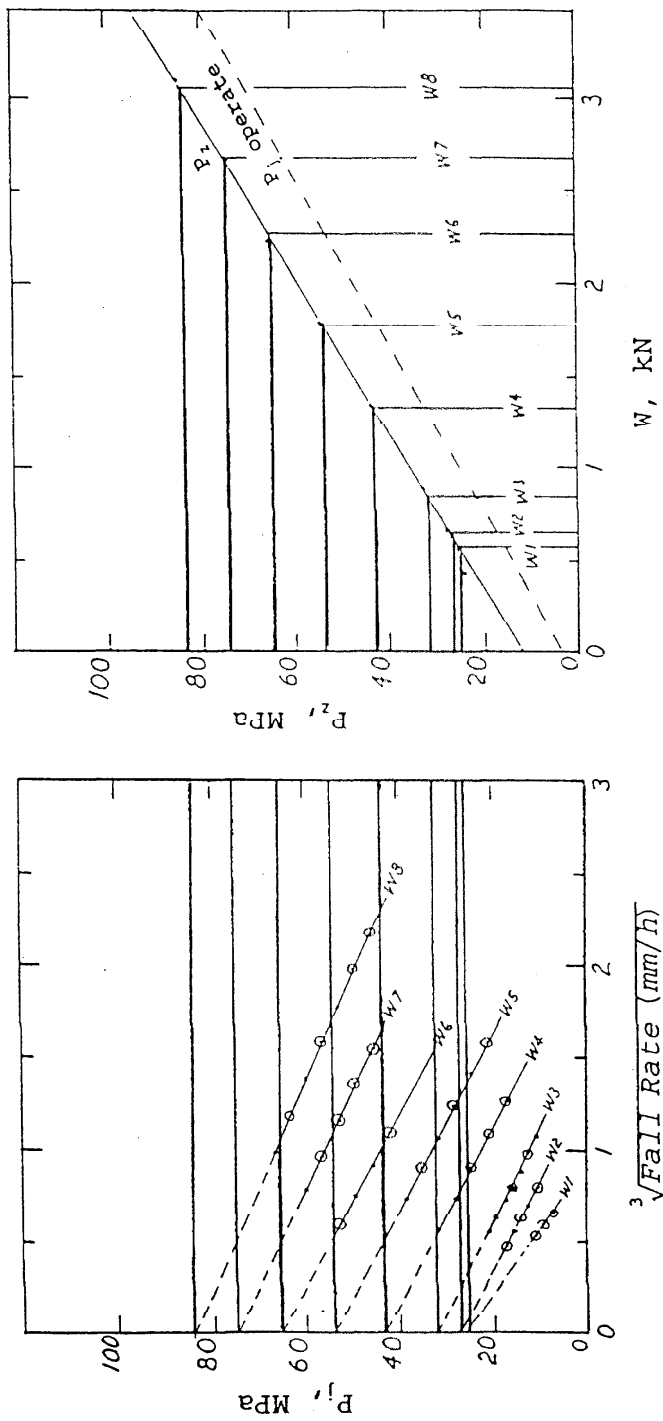


Figure 6. On the left, the cube root of the measured fall rate is plotted as a function of P_i for several loads. These lines are extrapolated to zero fall rate to determine the values of P_i . On the right, these values of P_i are plotted as a function of the load. The curve representing the values of P_i to be used in operating the piston gage is also shown as a function of the load.

p_j as a function of $(\partial s/\partial t)^{1/3}$ for each load W yielding a value of p_j for each W . Then to obtain an expression for interpolation, an expression of the form

$$P_z = P_{z0} + S_z W + Q_z W^2 \quad (18)$$

is fitted to the $p_z(W)$ data.

p_j and p_z are dependent upon the pressurizing fluid and must be measured for each fluid used.

C. Total Uncertainty of the Primary Standards.

As of 1 October 1992, the primary standard supporting the gas pressure calibration service is the NIST gas thermometer manometer (GTM). The primary standards for the oil pressure calibration service are three controlled-clearance piston gages. Identification numbers and pressure ranges are listed in table 3.

The uncertainty for the GTM over its pressure range is 2 ppm based on tripled standard deviations [1-4]. For the controlled-clearance piston gages, each of the parameters of eq (1) contributes to the overall uncertainty of the pressure calculation for these piston gages. The fractional uncertainty in p can be calculated from

$$\frac{dp}{p} = \left[\sum \left(\frac{1}{p} \frac{\partial p}{\partial x_i} dx_i \right)^2 \right]^{1/2} \quad (19)$$

where the x_i are the parameters of eq (1).

As the estimated uncertainties for some of the parameters increase as the pressure increases, it is customary to state the most pessimistic case, that is, the uncertainty at maximum pressure. Tables 4-6 list the values of the parameters of eq (1) required to specify the maximum pressure, the expressions and values for each of the normalized partial derivatives, the uncertainties in the measurement of the parameters, and the resulting relative pressure uncertainties for each of these controlled-clearance gages.

Table 3. NIST Primary Pressure Standards

<u>NIST designation</u>	<u>Pressure ranges</u> (MPa)	<u>Media</u>
GTM	0.01 to 0.13	gas
PG27	2 to 28	oil
PG20	30 to 140	oil
PG67	37 to 280	oil

Table 4. Pressure Uncertainty for PG27 at a Nominal 28 MPa

X_i	Value	$\frac{1}{P} \frac{\partial P}{\partial X_i}$	Value	$dX_i (1\sigma)$	$\frac{1}{P} \frac{\partial P}{\partial X_i} dX_i$, ppm
M	1.40×10^2 kg	1/M	7.14×10^{-3} /kg	2.8×10^{-4} kg	2.0
g	9.801018 m/s ²	1/g	1.02×10^{-1} s ² /m	5×10^{-6} m/s ²	0.5
ρ_a	1.18 kg/m ³	$1/\rho_m$	1.2×10^{-4} m ³ /kg	1×10^{-2} kg/m ³	1.2
ρ_m	8.4×10^3 kg/m ³	ρ_a/ρ_m^2	1.7×10^{-8} m ² /kg	0	0
γ	3.05×10^{-2} N/m	C/gM	1.82×10^{-5} m/N	3×10^{-4} N/m	0
C	2.5×10^{-2} m	γ/gM	2.22×10^{-5} /m	1×10^{-5} m	0
A_o	4.902139×10^{-5} m ²	$1/A_o$	2.04×10^4 /m ²	3.2×10^{-10} m ²	6.5
α_p	4.5×10^{-6} /°C	(T-T _r)	3 °C	3×10^{-7} /°C	0.9
α_c	4.5×10^{-6} /°C	(T-T _r)	3 °C	3×10^{-7} /°C	0.9
(T-T _r)	T _r = 23 °C	$\alpha_c + \alpha_p$	9×10^{-6} /°C	2×10^{-2} °C	0.2
b	-5.49×10^{-13} /Pa	p	2.8×10^7 Pa	1.8×10^{-14} /Pa	0.5
p	2.8×10^7 Pa	b	5.49×10^{-13} /Pa	1×10^5 /Pa	0.1
p_z	6.07×10^7 Pa	d	3.02×10^{-12} /Pa	1.5×10^6 Pa	4.5
d	3.02×10^{-12} /Pa	(p _z -p _j)	2.36×10^7 Pa	7.4×10^{-14} /Pa	1.7
p_j	3.71×10^7 Pa	d	3.02×10^{-12} /Pa	7.0×10^4 Pa	0.2
A*	ΔT	α_p	4.5×10^{-6} /°C	2.7×10^{-2} °C	0.1
A*	α_p	ΔT	3 °C	3×10^{-7} /°C	0.9

$$\frac{dp}{p} = 9 \text{ ppm}, (1 \sigma) \quad 3 \sigma = 27 \text{ ppm}$$

*Uncertainties due to changing the reference temperature from the 20 °C of the dimensional metrology laboratory to the 23 °C of the pressure measurement laboratory.

Table 5. Pressure Uncertainty for PG20 at Nominal 140 MPa

X_i	Value	$\frac{1}{P} \frac{\partial P}{\partial X_i}$	Value	dX_i (1 σ)	$\frac{1}{P} \frac{\partial P}{\partial X_i} dX_i$, ppm
M	4.60×10^2 kg	1/M	2.17×10^{-3} /kg	6.6×10^{-4} kg	1.4
g	9.801018 m/s ²	1/g	1.02×10^{-1} s ² /m	5×10^{-6} m/s ²	0.5
ρ_a	1.18 kg/m ³	1/ ρ_m	1.25×10^{-4} m ³ /kg	1×10^{-2} kg/m ³	1.3
ρ_m	8.0×10^3 kg/m ³	ρ_a/ρ_m^2	1.8×10^{-8} m ³ /kg	0	0
γ	3.05×10^{-2} N/m	C/gM	4.4×10^{-5} m/N	3×10^{-4} N/m	0
C	2.0×10^{-2} m	γ/gM	6.8×10^{-5} /m	1×10^{-5} m	0
A_o	3.218871×10^{-5} m ²	1/ A_o	3.11×10^4 /m ²	5.1×10^{-10} m ²	15.9
α_p	9.41×10^{-6} /°C	(T-T _r)	2 °C	3×10^{-7} /°C	0.6
α_c	9.41×10^{-6} /°C	(T-T _r)	2 °C	3×10^{-7} /°C	0.6
(T-T _r)	T _r = 23 °C	$\alpha_c + \alpha_p$	1.88×10^{-5} /°C	2×10^{-2} °C	0.4
b	-7.23×10^{-13} /Pa	p	1.4×10^8 Pa	2.2×10^{-14} /Pa	3.0
p	1.4×10^8 Pa	b	7.23×10^{-13} /Pa	1×10^2 /Pa	0.1
p_z	1.35×10^8 Pa	d	8.96×10^{-12} /Pa	3×10^6 Pa	2.6
d	8.96×10^{-12} /Pa	(p _z -p _j)	4.2×10^7 Pa	3×10^{-13} Pa	12.6
p_j	6.6×10^7 Pa	c	8.96×10^{-12} /Pa	5.9×10^4 Pa	0.5
A*	ΔT	α_p	9.41×10^{-6} /°C	2×10^{-2} °C	0.2
A*	α_p	ΔT	3 °C	3×10^{-7} /°C	0.9

$$\frac{dp}{p} = 20.7 \text{ ppm (1}\sigma\text{)} \quad 3\sigma = 62 \text{ ppm}$$

*Uncertainties due to changing the reference temperature from the 20 °C of the dimensional metrology laboratory to the 23 °C of the pressure measurement laboratory.

Table 6. Pressure Uncertainty for PG67 at Nominal 290 MPa

X_i	Value	$\frac{1}{P} \frac{\partial P}{\partial X_i}$	Value	dX_i (1 σ)	$\frac{1}{P} \frac{\partial P}{\partial X_i} dX_i$, ppm
M	418 kg	1/M	2.4×10^{-3} /kg	1.4×10^{-3} kg	3.4
g	9.801018 m/s ²	1/g	1.02×10^{-11} s ² /m	5×10^{-6} m/s ²	0.5
ρ_a	1.18 kg/m ³	1/ ρ_m	1.2×10^{-4} m ³ /kg	1.2×10^{-2} kg/m ³	1.4
ρ_m	8.4×10^3 kg/m ³	ρ_a/ρ_m^2	1.7×10^{-8} m ³ /kg	0	0
Y	3.05×10^{-2} N/m	C/gM	3.2×10^{-6} N/m	2×10^{-3} N/m	0
C	1.3×10^{-2} m	Y/gM	7.5×10^{-6} /m	1.3×10^{-6} m	0
A _O	1.4219412×10^{-5} m ²	1/A _O	7.03×10^4 /m ²	2.1×10^{-10} m ²	14.8
α_p	4.5×10^{-6} /°C	(T-T _r)	3 °C	7.5×10^{-8} /°C	0.2
α_c	4.5×10^{-6} /°C	(T-T _r)	3 °C	7.5×10^{-8} /°C	0.2
(T-T _r)	T _r = 23 °C	$\alpha_c + \alpha_p$	9×10^{-6} /°C	2×10^{-2} °C	0.2
b	-5.61×10^{-13} /Pa	p	2.8×10^8 Pa	1.8×10^{-14} /Pa	5.0
p	2.8×10^8 Pa	b	5.61×10^{-13} /Pa	1×10^5 Pa	0.1
P _Z	1.57×10^8 Pa	d	2.7×10^{-12} /Pa	5.7×10^5 Pa	1.5
d	2.7×10^{-12} /Pa	(p _Z -p _j)	1.16×10^8 Pa	1.58×10^{-13} /Pa	18.3
P _J	3.9×10^7 Pa	d	2.7×10^{-12} /Pa	3.5×10^4 Pa	0.1
A*	ΔT	α_p	4.5×10^{-6} /°C	2×10^{-2} °C	0.1
A*	α_p	ΔT	3 °C	7.5×10^{-8} /°C	0.2

$$\frac{dp}{p} = 24.4 \text{ ppm}, (1 \sigma) \quad 3 \sigma = 73 \text{ ppm}$$

*Uncertainties due to changing the reference temperature from the 20 °C of the dimensional metrology laboratory to the 23 °C of the pressure measurement laboratory.

The temperature of the NIST Dimensional Metrology Laboratory is maintained at 20 °C to match the temperature of the dimensional laboratories in European national standards laboratories. The NIST Pressure Measurement Laboratories are maintained at 23 °C to match the temperature most commonly found in U.S. industrial metrology laboratories. The last two entries in tables 4-6 marked (*) are the uncertainties due to changing the reference temperature from 20 °C to 23 °C.

The estimates for the uncertainties of each parameter (dx_i) are given as one standard deviation (1σ). These estimates come from a number of sources. In the case of M , g , α_p , and α_c , the estimates are provided by the laboratories that made the corresponding measurements. The uncertainty in ρ_a is estimated on the basis of the comparison in other laboratories of measurements with the calculations we have used. Since the controlled-clearance gages operate only in the gage mode and the identical values of ρ_m used by the mass laboratory in determining the true mass values were used for the air buoyancy correction, the uncertainty in ρ_m is zero. The measurements of γ are assumed to be accurate to within 10 percent. As previously mentioned, the uncertainty in A_o is based on judgment of the departure of the piston from a perfectly round and straight cylinder and on the quality of the dimensional measurement process. The uncertainty in the value of b is assumed to be within three percent. The uncertainty in $T-T_r$ is based on the calibration and location of the temperature probes. For p_z and d , the uncertainties are the standard deviations of the residuals from fitting empirical equations to the pertaining data. The calibration of the gage on the jacket pressure system gives rise to the uncertainty in p_j .

Each of these controlled-clearance standard piston gages has its own peculiarities that require some comment in addition to the data given in tables 4-6.

PG27

This gage represents a departure from the earlier design philosophy in that formerly the pistons and cylinders were usually custom made by outside contractors to NIST specifications. PG27

was designed around a commercially available piston and cylinder. Because of the required roundness and straightness of the piston and the cylinder bore and because of the small clearance between them, the manufacture of these parts demands great skill developed by long experience. Typically, a firm that produces excellent pistons and cylinders in a given material, geometry, and size cannot maintain that quality for a custom job wherein any of these three factors are changed until they have again developed the skill required by the new circumstances through long experience. Thus, custom designs of the highest quality are now far more expensive than commercially available designs of equal quality.

The piston and cylinder of PG27 were made of tungsten carbide. The mounting as a controlled-clearance piston gage is an NIST design employing as many commercially available parts as possible. Figure 7 is a diagram of PG27.

The values of d and p_z given in table 4 are appropriate for 28 MPa. For any pressure, d can be expressed by the empirical relation

$$d(\text{Pa}^{-1}) = 3.425 \times 10^{-12} - 2.974 \times 10^{-16} W$$

where W is in newtons. p_z is given by

$$p_z(\text{Pa}) = 4.013 \times 10^7 + 1.498 \times 10^4 W$$

PG20

PG20 is an NIST design and is shown in figure 8. In this case the piston and cylinder are made of tool steel. The unusual feature of this gage is the nonuniform wall thickness of the cylinder, the outer diameter of which was tailored in an attempt to obtain smoother and more uniform operation. As a result, d is an exponential function of W ,

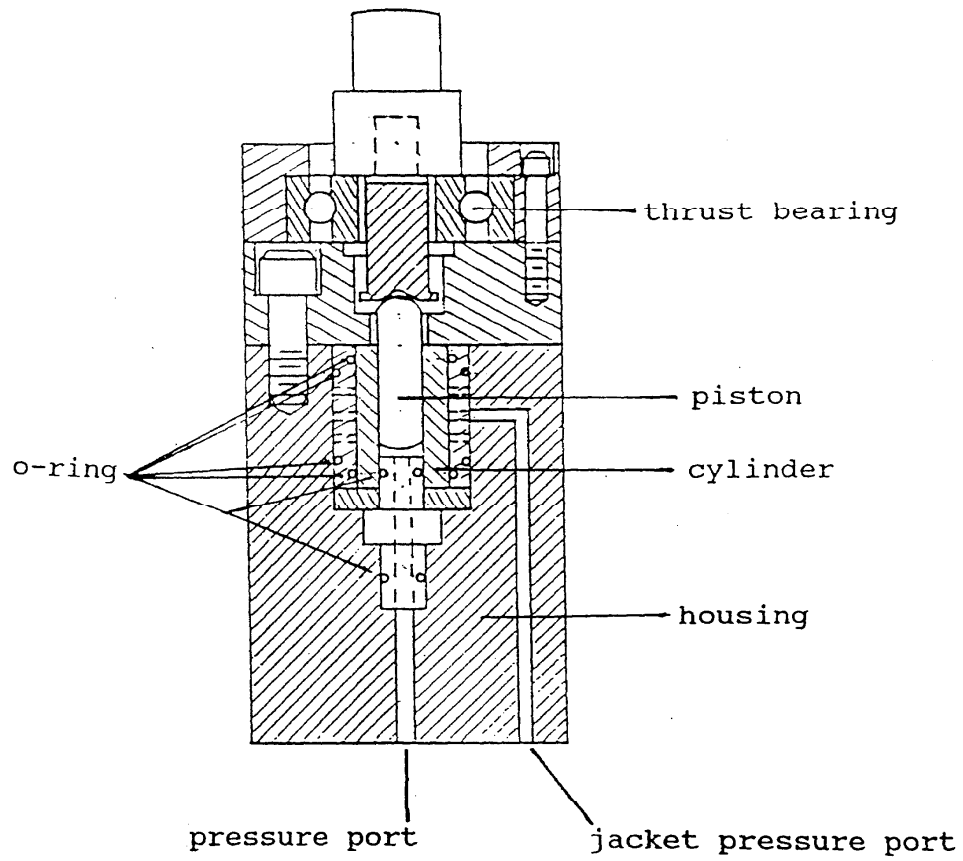


Figure 7. PG27 controlled-clearance piston gage.

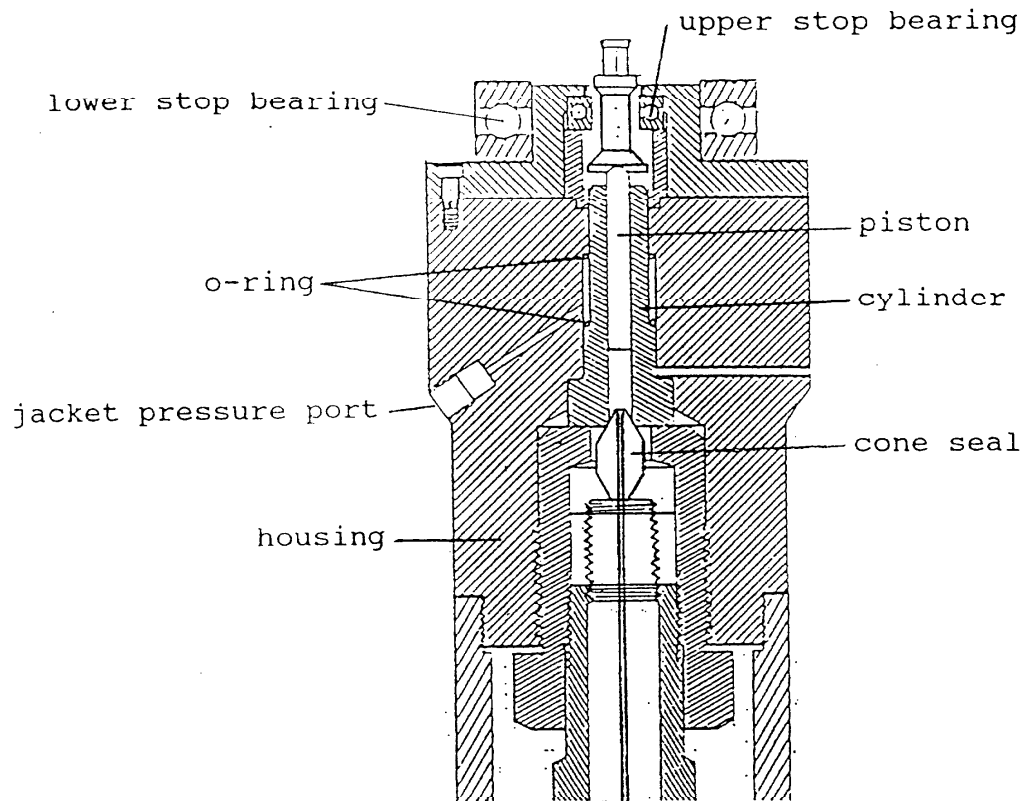


Figure 8. PG20 controlled-clearance piston gage.

$$d(\text{Pa}^{-1}) = 8.662 \times 10^{-12} e^{152.71W}$$

and

$$p_z(\text{Pa}) = 9.309 \times 10^6 + 2.620 \times 10^4 W - 0.8401 W^2$$

PG67

Like PG27, PG67 has a commercially available tungsten carbide piston and cylinder mounted as a controlled-clearance piston gage of NIST design. The mounting design incorporates as many commercially available parts as possible. It is shown in figure 9. For this gage,

$$d(\text{Pa}^{-1}) = 3.691 \times 10^{-12} - 2.470 \times 10^{-16} W$$

and

$$p_z(\text{Pa}) = 3.952 \times 10^7 + 2.965 \times 10^4 W$$

D. Transfer Standards and Their Uncertainty.

NIST controlled-clearance primary standard piston gages are used to calibrate NIST transfer standard piston gages which are then used to calibrate customers' gages. The NIST transfer standards are all unmodified, commercially available piston gages. Use of the transfer standards saves wear on the primary standards and saves time. The primary standards are generally used only for international intercomparisons, to calibrate the master gages for piston gage manufacturers, and to calibrate NIST transfer gages.

As of 1 October 1992, there are four transfer standards used in the gas calibration program and four for oil. Their NIST designations, pressure ranges and pressure media are listed in table 7.

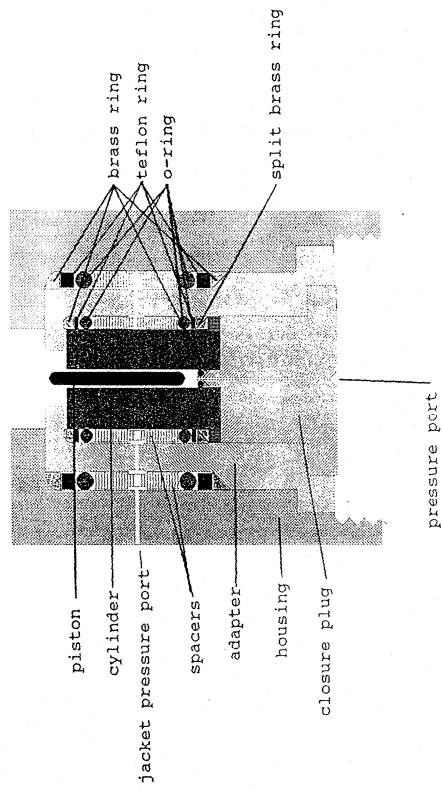


Figure 9. PG67 controlled-clearance piston gage.

Table 7. NIST Transfer Standard Piston Gages

<u>NIST designation</u>	<u>Pressure ranges</u>	<u>Medium</u>
PG22	7 to 105 kPa	gas
PG34	69 to 1370 kPa	gas
PG13	0.41 to 4.1 MPa	gas
PG23	0.7 to 17.3 MPa	gas
PG42	1.1 to 29 MPa	oil
PG6	7.2 to 104 MPa	oil
PG41	14 to 139 MPa	oil
PG21	13.8 to 276 MPa	oil

A transfer standard is calibrated against a primary standard using the cross-floating technique. To calibrate a piston gage is to determine its area as a function of pressure, known as the effective area, through pressure measurements. This is done by connecting both gages to a common pressure line, floating both pistons at their respective reference levels, and assuring both are in equilibrium. The process is repeated for several pressures. The effective area A_e of the transfer standard is calculated from the known weights on both gages and the known effective area of the standard. The details of this procedure are considered in the next section.

In general the effective area of a transfer standard can be expressed as

$$A_e = A_0 (1 + b_1 p_n + b_2 p_n^2) \quad (20)$$

where A_0 is the area at atmospheric pressure, b_1 and b_2 are the first and second order pressure coefficients, respectively, and p_n is the nominal pressure. The values of these coefficients and the total estimated uncertainties for the eight transfer standard gages are listed in table 8.

The basis for the total estimated uncertainty for the oil transfer standards is the sum of the estimated uncertainty (3σ) for the primary standard and the tripled standard deviation of the predicted values resulting from the least squares fit to the calibration data for the transfer standard.

The situation is somewhat more complicated for the gas transfer standards. The calibrations of the gas transfer standards are traceable to the GTM. The GTM was designed to operate only in the absolute mode. While the gas transfer standards can operate either in the gage or the absolute mode, the gas calibration service is operated in the gage mode. There is evidence to suggest that the effective area for a gas piston gage may not be identical in the two modes [12]. There is also a body of data that suggests the effective area of a gas piston gage also depends upon the gas used [12]. Both of these effects are under investigation. To establish the total estimated uncertainty for the gas transfer standards, we again sum the estimated uncertainty (3σ) for the

Table 8. Areas, pressure coefficients, and total estimated uncertainties of NIST pressure transfer standards

Gage	A_0, m^2	b_1	b_2	Uncertainty, ppm
PG22	3.357243×10^{-4}	0	0	Note 1
PG34	8.397343×10^{-5}	0	0	27
PG13	8.389264×10^{-6}	0	0	50
PG23	8.390322×10^{-6}	-1.48×10^{-12}	0	50
PG42	8.402138×10^{-5}	-2.4×10^{-12}	0	Note 2
PG6	1.679672×10^{-5}	-2.8×10^{-12}	0	77
PG41	1.680278×10^{-5}	-2.64×10^{-12}	0	79
PG21	8.402922×10^{-6}	-2.81×10^{-12}	0	85

Note 1. From 7 kPa to 34 kPa, 35 ppm.

From 35 kPa to 105 kPa, 22 ppm.

Note 2. From 1.1 MPa to 2 MPa, 86 ppm.

From 2 MPa to 2.3 MPa, 66 ppm.

From 2.3 MPa to 29 MPa, 60 ppm.

Note 3. All uncertainties are based on tripled standard deviations.

primary standard and the tripled standard deviation of the predicted values for the calibration of the transfer standards and then increased the sums enough to cover the upper limits of the mode and species-of-gas effects. We expect these uncertainties to be reduced as research progresses and we learn how to calculate and predict these two effects.

The calibration traceability of the transfer standards and various intercomparisons are shown by the diagram in figure 10. PG23 is a gas-operated gage. Both PG27 and PG6 operate with oil. Intercomparisons between PG23 and PG6 or PG27 were done using a gas/oil interface device.

E. Calibration Quality Control.

Primary pressure standards are characterized in terms of fundamental units, namely: mass, length, time, and temperature. Transfer standards are calibrated through pressure measurements against primary standards.

Confidence in the characterization of a primary standard can be derived through careful error analysis and by intercomparison with other primary standards characterized in other laboratories by other people. Such intercomparisons have been done with other national standards laboratories and are described in Section IV. International Intercomparisons.

Confidence in the stability over time of a primary standard can be achieved through periodic recharacterization or by periodic calibration of transfer standards and tracking the areas of the transfer standards as a function of time on control charts. If the areas of the transfer standards remain within acceptable limits over time, we can then assume both the primary and the transfer gages are stable. If the areas do not remain within acceptable limits, then we may need to recharacterize the primary standard in terms of fundamental units in an effort to identify the problem.

Figures 11-14 are control charts wherein the relative change of area with respect to the average has been plotted as a function of the calendar year in which the NIST pressure transfer standards were calibrated. There are no control charts for PG23, PG34, PC41,

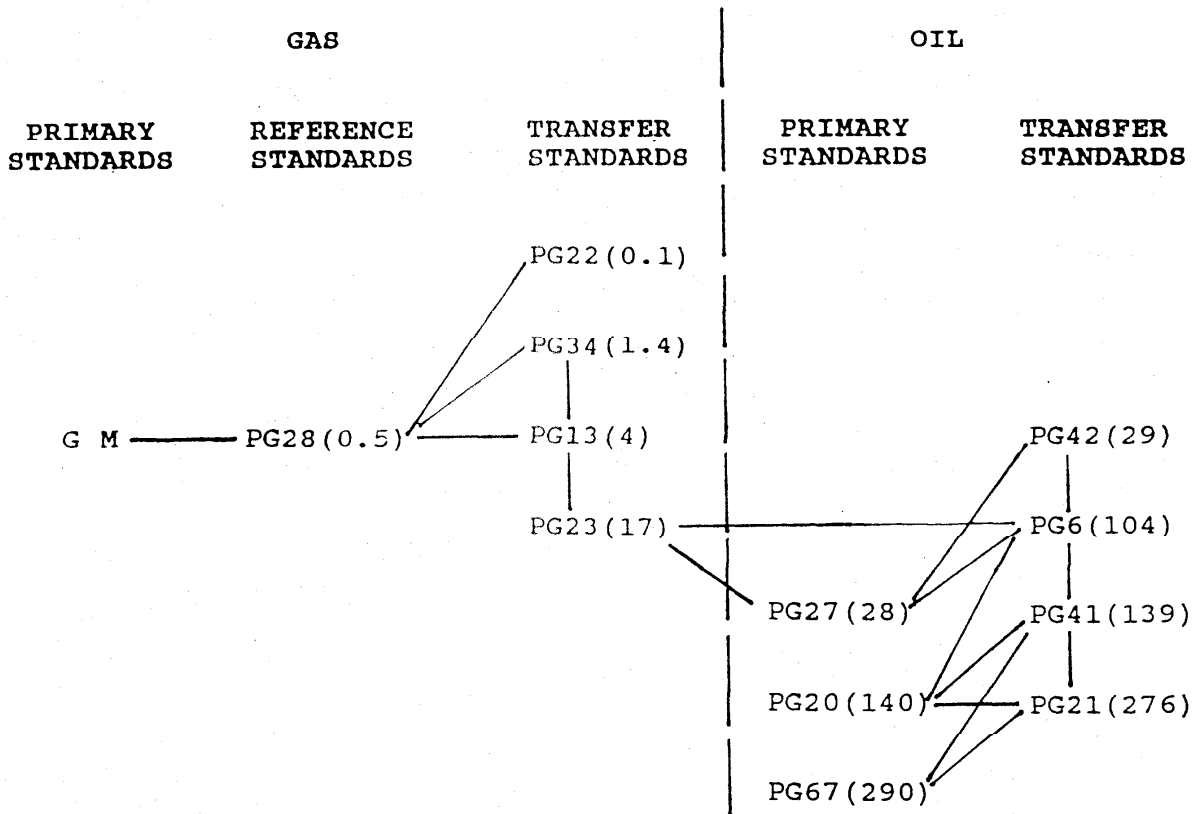


Figure 10. Intercomparisons involving NIST primary and transfer standard piston gages. The numbers in parenthesis are the maximum pressures of the gages expressed in MPa.

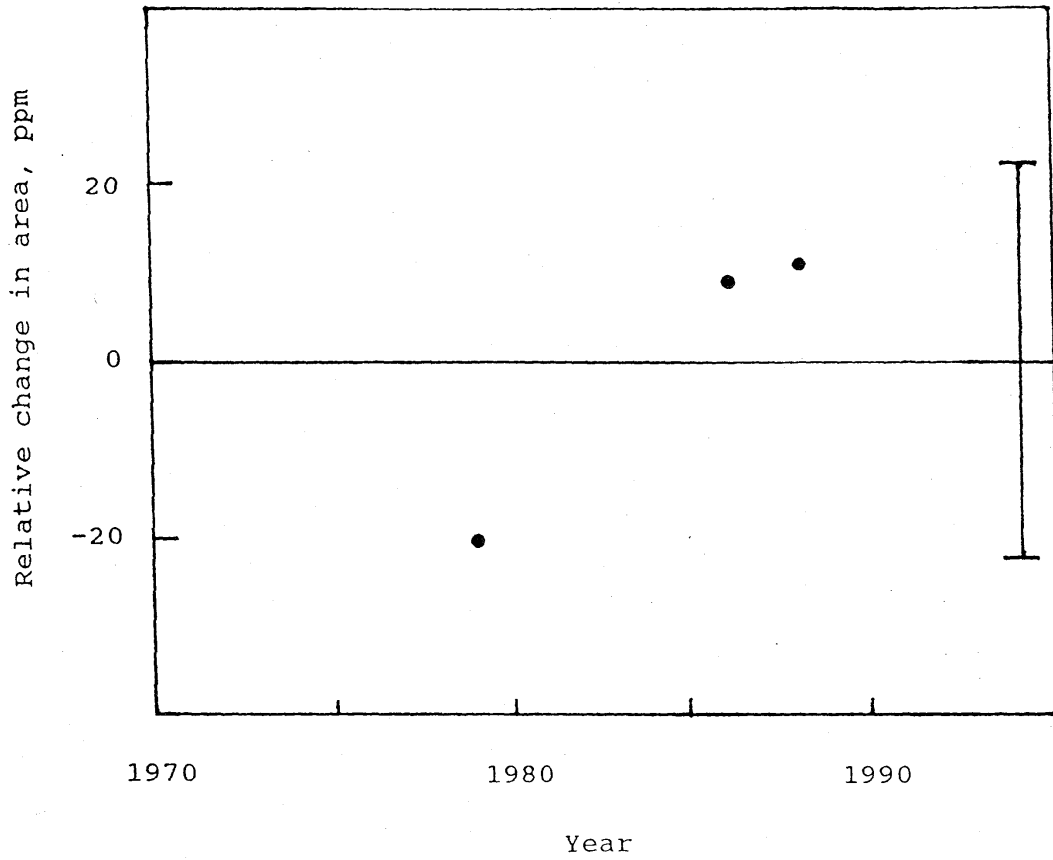


Figure 11. The relative change in the area with respect to the average (3.357205 E-4) for PG22 as a function of calendar year. The current total uncertainty at the maximum pressure is represented by the error bar at the right.

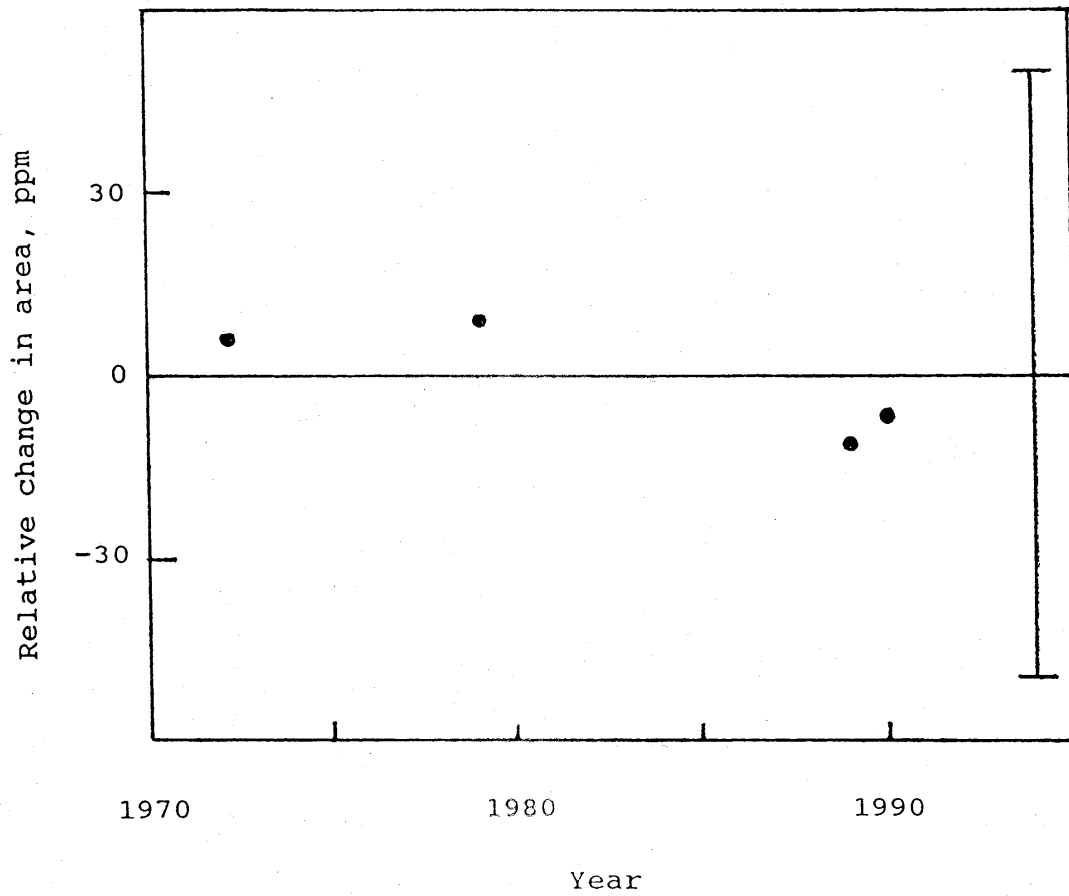


Figure 12. The relative change in the area with respect to the average (8.389305 E-6) for PG13 as a function of calendar year. The current total uncertainty is represented by the error bar at the right.



Figure 13. The relative change in the area at the maximum pressure with respect to the average ($1.679203 \text{ E-}5$) for PG6 as a function of calendar year. The current total uncertainty is represented by the error bar at the right.

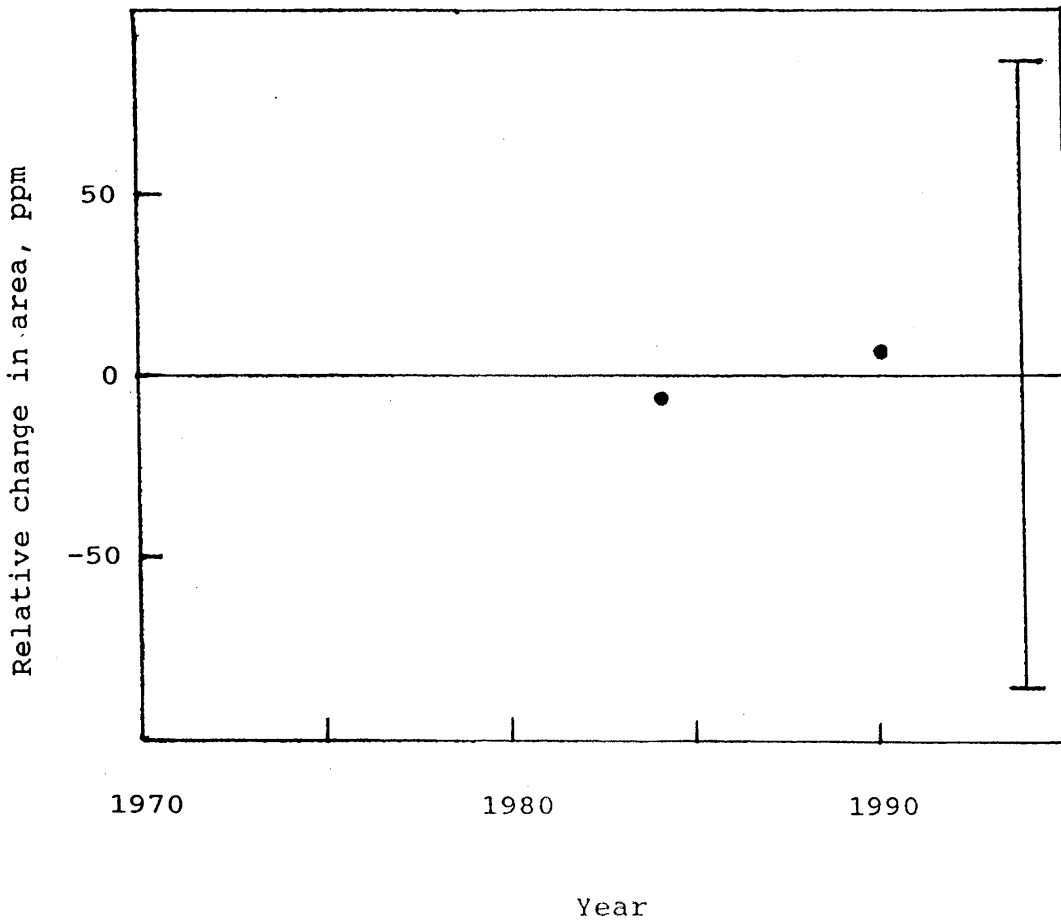


Figure 14. The relative change in the area at the maximum pressure with respect to the average (8.396495 E-5) for PG21 as a function of calendar year. The current total uncertainty is represented by the error bar at the right.

and PG42 as they are too new to have a recalibration history.

The recalibration schedule for a transfer standard is an open question which depends upon use, abuse, age of the gage, and the materials from which the piston and cylinder are made. It is generally accepted by the pressure metrology community that pistons and cylinders made of tungsten carbide are stable and a recalibration cycle of a few years is appropriate. However, such is not the case for steel. There is a report of a new steel piston in a tungsten carbide cylinder that increased in area by 24.6 ppm over a period of 15 months and by an additional 9.6 ppm during the next 21 months suggesting the area was becoming asymptotically stable with time [13]. The suggested cause was the relieving over time of strains induced by the manufacturing process. Clearly, such a unit would warrant frequent recalibration until one became confident of the stability.

III. CROSS-FLOAT CALIBRATION TECHNIQUE

In principle, we can determine the area and the pressure coefficient of a piston gage from measurements of the internal diameter of the cylinder, the diameter of the piston and a computation of the pressure coefficient using elastic distortion theory. However, the resulting uncertainties are so large that in practice piston gage calibrations are done by cross-floating against a standard.

For this technique, both piston gages are connected to a common pressure line along with an appropriate pressure generator. The effective area, A_e , of the test gage is

$$A_e = F/p \quad (21)$$

where p is the pressure generated at the reference level of the test instrument by the standard gage and F is the force exerted on the piston of the test gage which is

$$F = \frac{Mg[1 - (\rho_a/\rho_m)] + \gamma C}{1 + (\alpha_p + \alpha_c)(T - T_r)} \quad (22)$$

For simplicity, the temperature correction of the area has been included with the force. The two gages are brought into pressure equilibrium by adjusting F and then A_e is calculated by eq (21). Values of A_e are thus determined over the entire operating pressure range of the test gage. The effective area at atmospheric pressure, A_0 , and the coefficients b_1 and b_2 can be obtained by fitting

$$A_e = A_0(1 + b_1P + b_2P^2) - t/P \quad (23)$$

to the $A_e(p)$ data obtained from the cross-float measurements. t is a tare that may indicate an error in the data or may be a property of the gage.

A. Experimental Arrangement.

It is essential that the pistons be vertical so that the force due to the weights is totally supported by the fluid under the piston and no component of the force is supported by the cylinder wall. Manufacturers usually mount levels on the piston gage base, provide leveling screws, and assure that the piston is normal to the base. With many designs a level can be temporarily placed directly on the top of the cylinder.

The pressure connections for a cross-float are shown schematically in figure 15. The test instrument (A) is connected to the standard (B) through a short length of tubing. A valve (C) can interrupt this connection. The differential pressure indicator (D) can be by-passed by valve (E). Valve (G) connects to the fluid supply consisting of a screw pump (H), gage (K) and reservoir (P). If a controlled-clearance piston gage serves as the standard, a separate supply of jacket pressure is required. Valves (C) and (E) must be constant-volume valves. Markus [14] has developed a pneumatically operated constant-volume valve that has been used at pressures up to 420 MPa and gives very satisfactory service. The differential pressure indicator should have a sensitivity of at least one part in one million and should be rugged enough to withstand the full line pressure applied differentially without

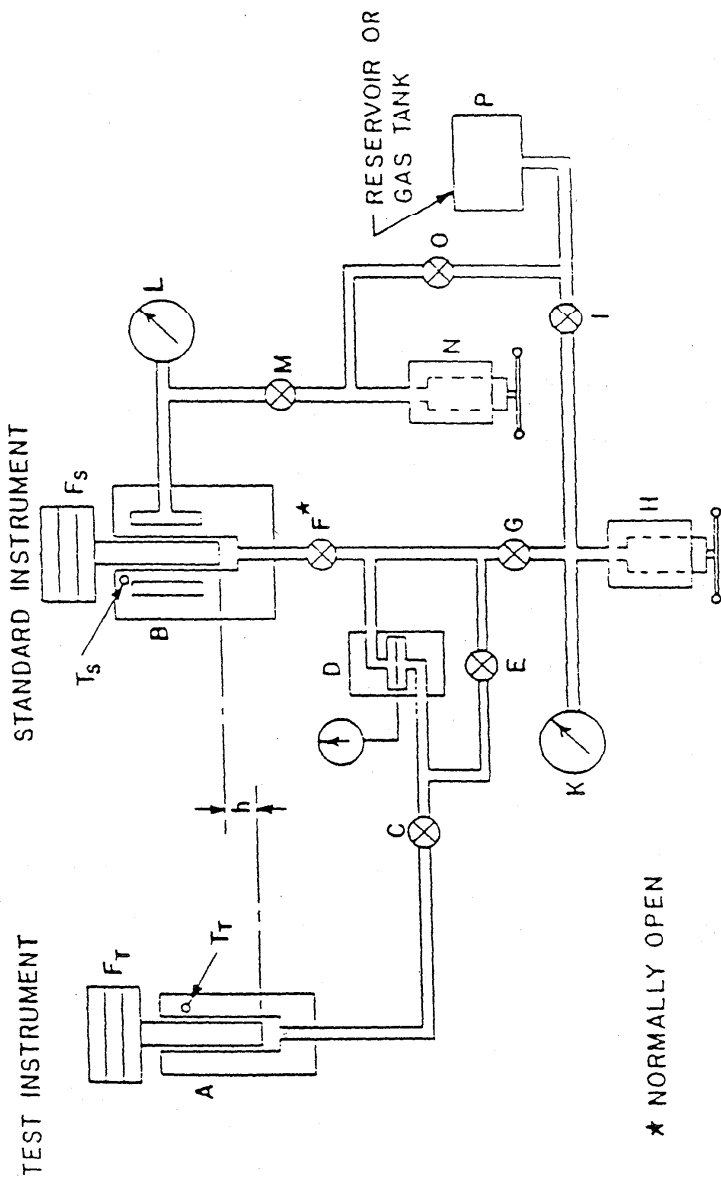


Figure 15. Schematic diagram of the connections for cross-float measurements.

damage.

Generally, to calibrate a piston gage using cross-float techniques, the NIST practice is to make ten measurements at seven pressures ranging from about ten percent of the full range to the full range, alternating the direction of rotation of the two instruments as shown in table 9. A list of weights to be used on both gages is prepared in advance and if a controlled-clearance gage is used, the appropriate operating jacket pressures are chosen from the plot of jacket pressure as a function of the cube root of fall rate with load as parameter, such as figure 6.

With valves (C) and (E) open and the weight hangers down on the stops, both gages are loaded and spun. We prefer to spin gages by hand and allow them to coast to avoid possible vertical force components resulting from continuous motor drives. Both pistons are then raised above their operating level by means of the screw pump (H) and left coasting with valve (G) closed until both gages have reached temperature equilibrium. With valve (C) closed the differential pressure indicator is zeroed by opening valve (E) and making the necessary electrical/mechanical adjustments to the indicator. Valve (E) is closed and (C) opened, and the weights on the test gage are adjusted to zero differential pressure. When balance is attained, the applied loads, the jacket pressure, and the gage temperatures are recorded. Finally valves (E) and (G) are opened and the pressure is lowered to bring the weight hangers down to the bottom stop before loading up for the next point.

The function of the differential pressure indicator is to detect when the two gages are in pressure equilibrium. While the indicator is convenient, it is not essential. Equilibrium can be determined by making fall rate measurements. For this technique the plumbing system is modified by replacing the differential pressure indicator with a pressure line and removing the bypass line and valve. The connection between the two gages now is simply a pressure line with a constant-volume valve so each gage can be isolated such that the only fluid loss for each gage is that bypassing its own piston. With this valve open, the gages are loaded with appropriate weights to bring the gages near to equilibrium. Then with the valve closed the fall rate of one of the gages is measured as the piston is falling through the

Table 9. Schedule of points taken during a cross-float calibration of a piston gage.

Point	Pressure	Direction of rotation	
	% of full range	standard	test
1	10	CW	CW
2	10	CW	CCW
3	40	CW	CW
4	70	CW	CCW
5	100	CW	CW
6	100	CCW	CCW
7	85	CCW	CW
8	55	CCW	CCW
9	55	CCW	CW
10	25	CCW	CCW

reference level. The weights on the test gage are then adjusted until the fall rate is unchanged whether the valve is open or closed. This is the equilibrium condition.

There are a variety of ways of making the fall rate measurements. A convenient method is to use commercially available proximity indicators specifically designed for the purpose. Another way is to use the capacitance proximity sensor-strip chart recorder system described above and observe the slope of the recorded trace as the valve is opened when the falling piston reaches the reference level. If the slope does not change, the two gages are in equilibrium. A more cumbersome method is to use a cathetometer and a stop watch. Whatever the choice of fall rate measurement apparatus, it must not add any unknown vertical forces to the pistons.

B. Reference Levels.

For piston gages with straight pistons, the reference level is normally defined as the lower end of the piston. For pistons with an irregular shape of the submerged part, an adjustment of the reference level is made as illustrated in figure 16. In this example the piston has a flange at the lower end serving as a stop. The volume of the shaded part of the flange is

$$V = (h\pi/4) (D^2 - d^2) \quad (24)$$

If the piston were lengthened such that the volume produced by the additional length was equal to the volume given by eq (24), the length of the piston would increase by

$$L = \frac{(D^2 - d^2) h}{d^2} \left(\frac{\rho_L}{\rho_m} \right) \quad (25)$$

where ρ_L/ρ_m is the ratio of the density of the metal in the shaded area of figure 16 to the density of the metal in the nonshaded area. The reference level for a piston of this shape would be defined as being L below the bottom of the piston.

In a piston gage cross-float, or whenever a piston gage is

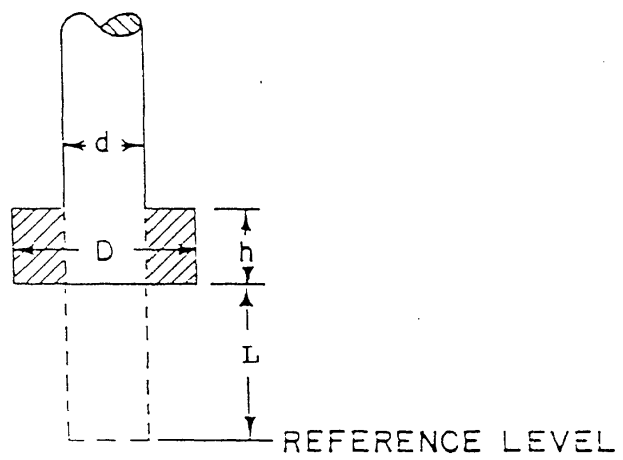


Figure 6. Adjustment of reference level for irregularly shaped pistons.

used to generate a known pressure at the reference level of another instrument, a correction has to be made for the fluid head in the connecting line. This correction can be expressed as

$$\beta = gH[\rho_{fl}(1 + p\kappa) - \rho_{air}] \quad (26)$$

where g is the acceleration due to gravity, H is the vertical separation between the reference levels, ρ_{fl} is the density of the pressurizing fluid, p is the pressure, κ is the compressibility of the fluid, and ρ_{air} is the density of the air. β is subtracted from the pressure generated by the standard instrument at its reference level. The level difference, H , is counted positive upwards from the reference level of the standard instrument. The term $1 + p\kappa$ corrects for the change of density of the fluid with pressure. The term $-\rho_{air}gH$ is the head correction due to atmospheric air density and is used only when the piston gage is operated in the gage mode.

C. Connections.

When connections are made in a pressure system, care should be taken to install the properly rated tubing, fittings, valves, etc. Plumbing material should be chosen to be fully compatible with the pressure fluid. Stainless steels are widely used in liquid systems, whereas copper, plastics, rubber, etc., are commonly found in low pressure gas systems. When threading and coning high pressure tubing, it is essential that the threads be carefully made and that cones have the correct angle and proper finish.

All plumbing should be carefully cleaned. If filters are used in a system, it is necessary to choose a type that will not break up or expel particles into the pressure fluid.

To obtain the optimum in response time, lines are usually kept short and internal diameters should be as large as is practicable. Damping of a system, if necessary, may be achieved through the use of needle valves, filters or other types of line restrictions.

Proper valve arrangement can make a system highly efficient and more than one type of valve may be useful. A constant volume valve, which operates without disturbing the internal pressure of the system, is a great advantage when used as the isolation valve

between two piston gages in a cross-float situation. Damping valves may be employed in a piston gage intercomparison set-up where short or long-term oscillations have been detected. Response time may suffer as a result of using damping valves, but this situation may be acceptable if the system is made more stable by using the valves. Nonrotating stem valves offer the advantage of long valve seat life.

D. Cleaning.

As in most high precision set-ups containing mechanical components with moving parts, a clean system is necessary. The oil piston gage will function properly over a longer period of time if the instrument, lines, and fittings are carefully cleaned. Damage can result if particles of dirt become lodged between the piston and cylinder. Oil piston gages should be cleaned with appropriate solvents whenever a change is made from one oil to another.

Gas piston gages will not function properly when dirty and if forced to operate under such conditions, damage to the piston and cylinder is likely.

To obtain the highest performance from a gas piston gage, a good cleaning technique is essential. One method is to use mild soap and warm water. The piston and cylinder should be scrubbed thoroughly, rinsed with warm water, air blasted to remove the water droplets and finally polished with lens tissue. Before assembling the piston and cylinder, dry, clean air (or nitrogen) is used to remove lint particles. The important points in a good cleaning technique are: (1) remove all foreign material, such as dirt, grease, and fingerprints, (2) leave no residue, (3) polish, (4) remove all remaining lint before assembling. It may be necessary to repeat the cleaning procedure to obtain satisfactory results. The only way to judge how clean is "clean enough" is by the performance of the gage. If the gage is clean, floating, and rotating (by hand) on the order of 30 revolutions per minute, it should take a few minutes to coast to a gradual stop. It is also important that the remaining plumbing be clean.

Where the removal of the cylinder is difficult or undesirable,

it must be cleaned in place. Water should be used with extreme care. It is far safer to use a solvent that will evaporate fairly rapidly.

The piston gage operator should be able to determine from the behavior of the instrument (spin time, sensitivity, etc.) whether the instrument is functioning properly. Proper operating specifications should be available from the operators manual provided by the manufacturer.

E. Rotation.

In most piston gages an electric motor is provided to rotate either the piston or the cylinder to relieve friction and to maintain a continuous film of gas or oil between piston and cylinder. Heat given off by some drive motors may increase the temperature of the piston and cylinder above the nominal room temperature over a period of several hours. Under these conditions it is difficult to measure the temperature of the piston and cylinder accurately. Shielding the motor or moving it to a different location may mitigate the problem.

Some commercial units have drive motors which rotate the piston assembly much faster than is necessary. High speed rotation of a gas gage can increase the danger of damage. Some manufacturers recommend the application of a thin film of oil to the piston and cylinder to prevent galling and to reduce excessive fall rates. While this procedure may lead to an acceptable fall rate, it will increase friction and reduce sensitivity. Some piston assemblies are rotated by threads attached to a drive mechanism. Unknown vertical forces will be applied to the piston if these threads are not kept horizontal when the gage is in operation. Hand rotation of the piston and weight stack is quite satisfactory since the optimum speed of rotation can be achieved for each instrument. A rate of 15 to 20 revolutions per minute is adequate for most gages.

F. Data evaluation.

We determine the effective area and the coefficients of the test gage by fitting eight equations to the calibration data and

then selecting that which is most appropriate. These equations are variations of eq (23) and are given below.

$$A_e = A_0 \quad (27.1)$$

$$A_e = A_0 - t/p \quad (27.2)$$

$$A_e = A_0(1 + b_1p) \quad (27.3)$$

$$A_e = A_0(1 + b_1p) - t/p \quad (27.4)$$

$$A_e = A_0(1 + b_1p + b_2p^2) \quad (27.5)$$

$$A_e = A_0(1 + b_1p + b_2p^2) - t/p \quad (27.6)$$

$$A_e = A_0(1 + b_2p^2) \quad (27.7)$$

$$A_e = A_0(1 + b_2p^2) - t/p \quad (27.8)$$

t may be either a tare error in the data that requires investigation or a coefficient necessary to characterize the behavior of the gage. At low pressures, the terms involving the pressure coefficients b_1 and b_2 are usually insignificant and either eqs (27.1) or (27.2) is used to characterize the gage. At high pressures the coefficient b_1 and occasionally also b_2 become significant and must be included in the function fitted to the data. In some cases, the coefficient b_1 is insignificant while b_2 is significant.

The computer program used for these computations provides, in addition to the coefficients, the standard deviations of the coefficients, the residuals, the standard deviations of the residuals, and the standard deviations of the predicted values. A plot of the residuals as a function of pressure will show whether any gross errors have been made in recording and entering the data and is a valuable aid in judging which equation is appropriate. One may also separate the data according to the direction of rotation of either gage and check for effects depending on the direction of the rotation.

Selecting the proper fit is a matter of judgment based on the

residuals, the standard deviations of the residuals, the standard deviations of the coefficients, and the standard deviations of the predicted values of the coefficients. The technique is to find the fit having no evident systematic structure in the plot of the residuals as a function of pressure, having the minimum standard deviation of the residuals, having the minimum standard deviation of the predicted values of the coefficients, and having no coefficient that is smaller than its corresponding tripled standard deviation. When these conditions do not exist for the same fit, then it is a matter of judgement and compromise. If two fits represent the data equally well, we would choose the simpler equation.

Our practice is to express the total uncertainty of the effective area for the test gage as three times the sum of the standard deviation of the predicted values for the chosen fit plus the estimated uncertainty (3 σ) of the effective area of the standard.

An example of a typical calibration report is in the Appendix.

IV. INTERNATIONAL INTERCOMPARISONS

A primary pressure standard must be characterized in terms of the fundamental units of mass, length, time and temperature, in contrast to a secondary standard or transfer standard that is calibrated through pressure measurements using the primary standard. An excellent way to test the quality of the characterization of a primary standard is by comparing it by direct pressure measurement with primary standards characterized by other personnel in other laboratories.

Two international intercomparisons of current NIST primary pressure standards have been done which include a bilateral intercomparison of gas gages with Istituto de Metrologia "G. Colonnetti" (IMGC)[15] and a round-robin intercomparison of oil gages sponsored by Bureau International des Poids et Mesures (BIPM)[13,16].

A. IMGC

Intercomparisons of pressures generated by a primary standard gas piston gage (IMGC5) of the Istituto di Metrologia "G. Colonnetti" were made with pressures generated by a transfer gas piston gage (PG23) of NIST and a primary standard gas piston gage (PG24) of NIST. PG 24 has since been retired.

IMGC5 is a simple piston and cylinder in which the area at atmospheric pressure (determined from the average of the areas of the piston and of the cylinder) was obtained from direct dimensional measurements of the diameters. The pressure coefficient of the area was determined by IMGC by comparison with another IMGC simple piston and cylinder gas piston gage of 2 MPa range whose pressure coefficient had been calculated theoretically. PG23 has a pressure range of 0.7 to 17.2 MPa and was calibrated against the primary standard PG24, but only over the range of 0.7 to 1.9 MPa. PG24 was a primary standard gas-operated, controlled-clearance piston gage with the area derived from dimensional measurements of the piston only, with an empirically determined correction based on extrapolation of jacket pressure required to close the cylinder on the piston, and a theoretical pressure coefficient applied to the deformation of the piston only.

A total of 21 comparisons at 10 different pressures was made between IMGC5 and PG23. Nitrogen was the pressurizing fluid for all of the measurements. All of the measurements were done in the gage mode. One method of evaluating the data was to regard PG23 as the standard and IMGC5 as a test gage to be calibrated and apply the usual NIST computer program to determine the areas of IMGC5. This program determines the effective area and the pressure coefficient of the test gage in terms of those of the standard.

The lowest order equation, eq (27.1), was selected and gives an effective area of the IMGC gage of $2.000661 \times 10^{-4} \text{ m}^2$ at 23 °C with a standard deviation of the area of 0.6 ppm. The area of the IMGC gage given by IMGC is $2.000662 \times 10^{-4} \text{ m}^2$ at 23 °C. The areas are seen to differ by 0.5 ppm which is less than one standard deviation.

Another method of evaluating the intercomparison was to calculate the pressure generated by each piston gage according to the method used by the respective laboratories. The pressures were referenced to the base of the IMGC piston to account for head

corrections. The average of the pressures calculated by IMGC minus the pressures calculated by NIST is -12.7 Pa with a standard deviation of the mean of 2.0 Pa. The average of the pressures calculated by IMGC minus the pressures calculated by NIST divided by the NIST pressure is -5.4 ppm with a standard deviation of the mean of 1.0 ppm.

Sixteen comparisons were made between IMGC5 and PG24 at five different pressures. The same equation (eq (27.1)) was selected for this pair of gages. It gives an effective area of the IMGC gage of $2.000649 \times 10^{-4} \text{ m}^2$ at 23 °C with a standard deviation of the area of 0.6 ppm. The difference in area of the IMGC gage determined by PG24 in this comparison with that given by IMGC is -6.5 ppm. The second method of evaluating the intercomparisons was also applied to this pair of gages. The average of the pressure calculated by IMGC minus the pressures calculated by NIST is -6.8 Pa with a standard deviation of the mean of 1.1 Pa. The average of the pressures calculated by IMGC minus the pressures calculated by NIST divided by the NIST pressures is -6.5 ppm with a standard deviation of the mean of 0.6 ppm.

Figure 17 is a plot of the differences in pressure calculated from the characteristics of the gages versus pressure, and figure 18 is a plot of the relative difference in pressure calculated from the characteristics of the gages versus pressure. While a systematic difference in pressure is evident in the data, it is small compared to the estimated systematic uncertainties.

Both methods of expressing the results of the intercomparisons show significantly better agreement between the gages (1 to 7 ppm) than the estimated systematic uncertainty of each of the gages (IMGC5, 24 ppm; PG23, 30 ppm; and PG24, 28 ppm).

The differences observed between IMGC5 and PG24 (the primary standard), 6.8 ppm by area comparison and 6.5 ppm by pressure comparison, indicate that the two different methods of calculating areas are well verified at this pressure range. The differences observed between IMGC5 and PG23 (the transfer standard), 0.5 ppm by area comparison and 5.4 ppm by pressure comparison, indicate that the latter gage serves very well as a transfer standard in the given pressure range.

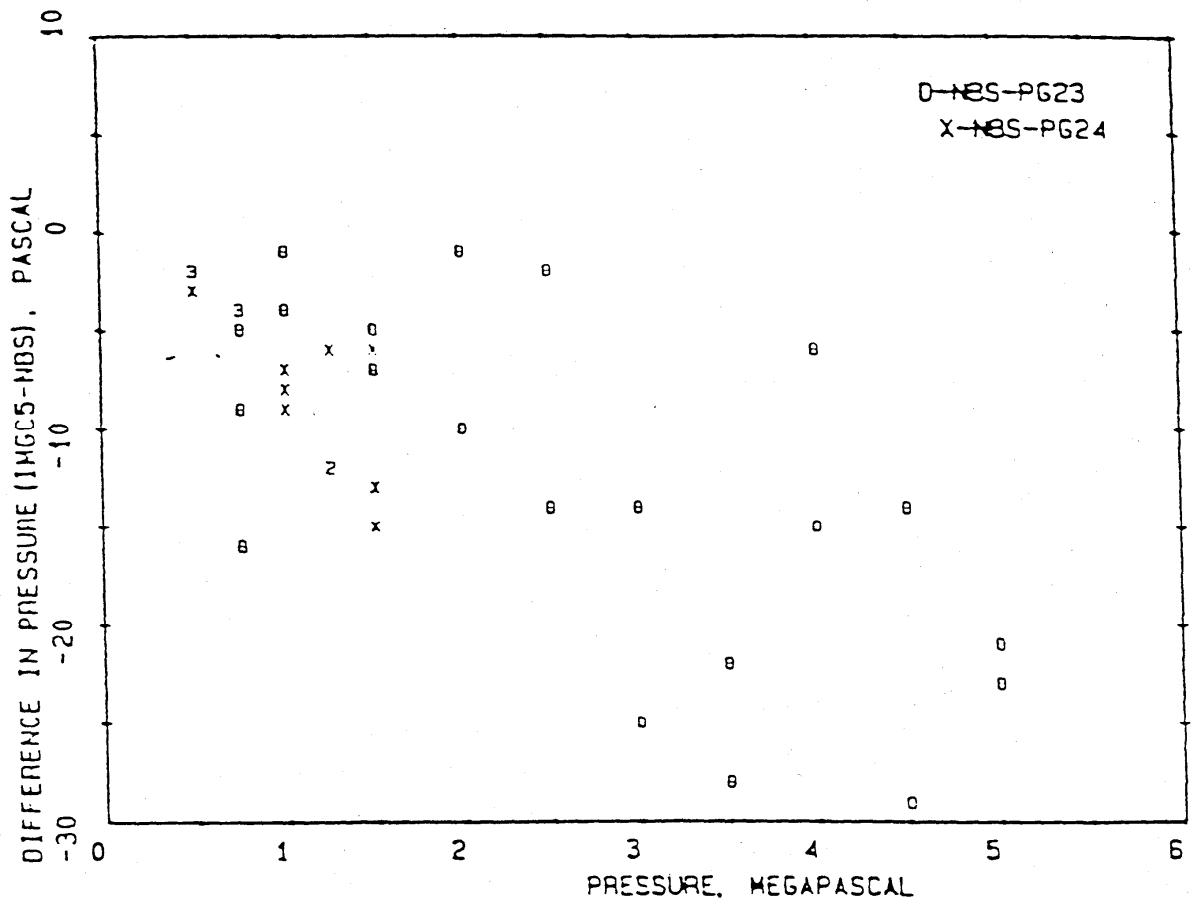


Figure 17. Difference in pressure (Pa) versus pressure (MPa) for IMGC5 against PG23 and IMGC5 against PG24. The numbers "2" and "3" represent the number of replicate data for IMGC5 against PG24 plotted at the same point.

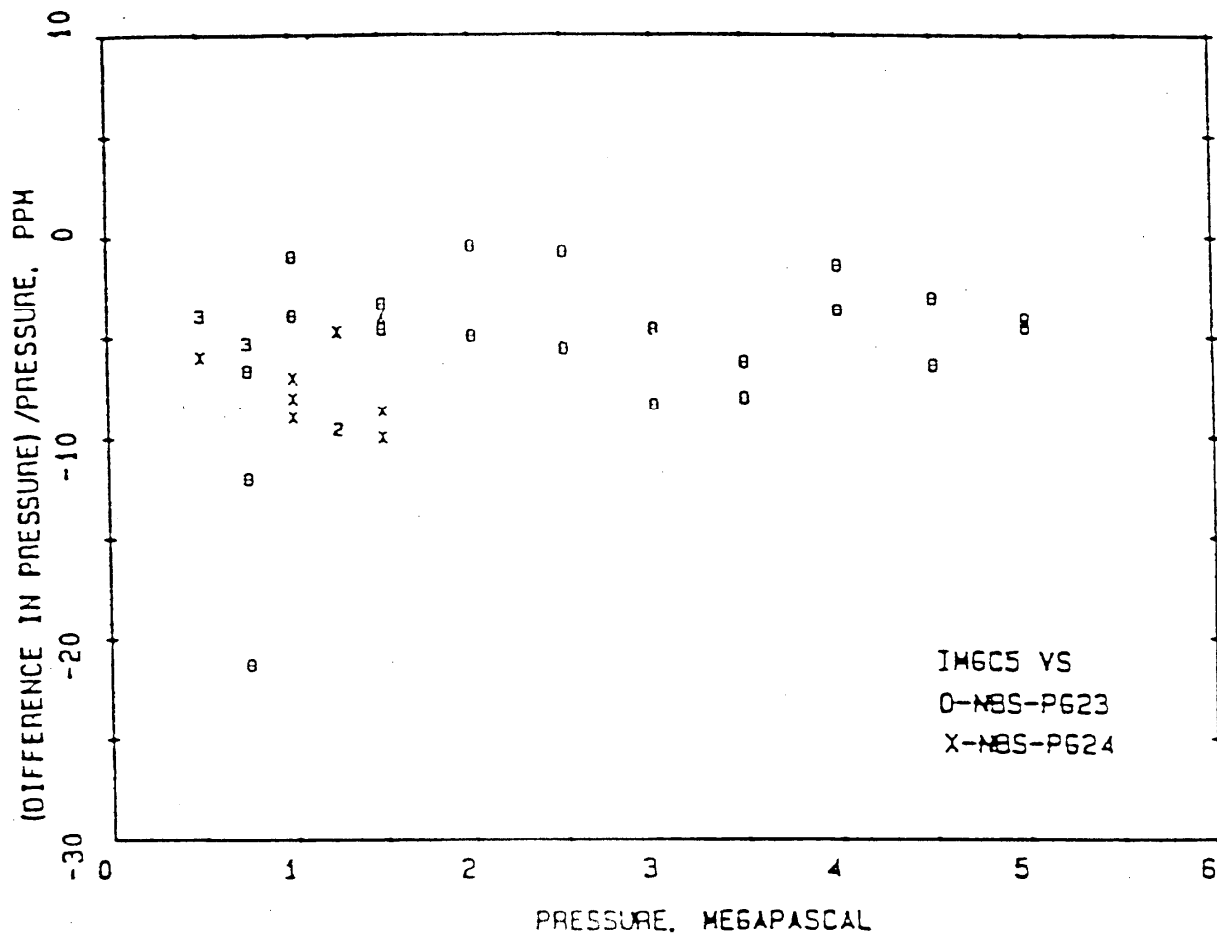


Figure 18. Difference in pressure divided by pressure (ppm) versus pressure (MPa) for IMGC5 against PG23 and IMGC5 against PG24. The numbers "2" and "3" represent the number of replicate data for IMGC5 against PG24 plotted at the same point.

B. BIPM

The Working Group on High Pressure of the Comité Consultatif pour la Masse et les Grandeurs Apparentées of the Bureau International des Poids et Mesures (BIPM) organized an intercomparison of the primary standard piston gages of 13 nations in the range of 20 to 100 MPa [13, 16]. The intercomparison was accomplished by circulating a transfer standard piston gage among the participating laboratories where each calibrated it using their primary standard. The data was then sent to the pilot laboratory for analysis. This was done in three phases. The participants on the first phase were Laboratoire National D'Essais (LNE), Paris, France, which is also the pilot laboratory; Istituto di Metrologia "G. Colonnetti" (IMGC), Torino, Italy; Physikalisch-Technische Bundesanstalt (PTB), Braunschweig, West Germany; National Physical Laboratory (NPL), Teddington, United Kingdom; and National Bureau of Standards (NBS, now National Institute of Standards and Technology, NIST), Gaithersburg, MD, USA. The results of the first phase shown in figure 19 are very instructive. This is a plot of the relative change of area of the transfer standard as a function of pressure as determined by each laboratory and compared to a reference value determined by the pilot laboratory. The curve for NIST is 14 ppm lower than that published in references. 13 and 16 due to improved thermal expansion data for the piston that was not available earlier.

Three features of figure 19 to note are:

1. The maximum spread in the data is 78 ppm which occurs at the maximum pressure. This is within the combined uncertainties of the laboratories and is very good agreement.

2. The area of the transfer standard increased by nearly 25 ppm during the year required for these measurements as indicated by the difference on the curves LNE1 and LNE2 obtained before and after circulation to the other laboratories. The transfer standard has a steel piston and a tungsten carbide cylinder. If we assume the total change was in the piston, then the corresponding change in the radius is 60 nm. It has been suggested that the increase in area is due to relaxation of stresses due to manufacture. Reference 13 is the first published report of this phenomenon. It requires further study to be understood. It should not be ignored.

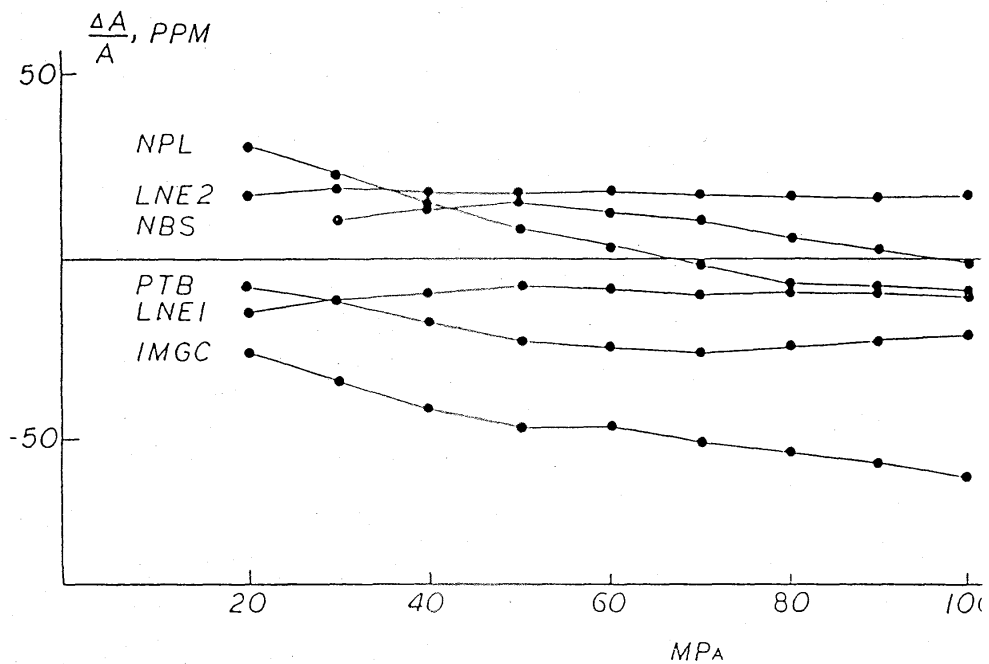


Figure 19. Relative change of the area of the transfer standard as determined by five national standards laboratories and plotted as a function of pressure.

3. The slopes of the curves are different which means that the various national laboratories do not agree on how the effective area of the transfer standard changes with pressure.

The differences in the results from various laboratories are better shown by fitting an equation of the form

$$A_e = A_0(1 + bp) \quad (28)$$

to the data from each laboratory and plotting the residuals as a function of pressure as has been done in figure 20. Three of the curves, NPL, PTB, and IMGC are concave upward. NPL determined the pressure coefficient of their standard using the "similarity" method [17] wherein two gages of identical geometry, but made of material having different known elastic moduli are cross-floated, providing data from which the distortion coefficient was calculated. Both PTB and IMGC calculated the distortion coefficient using elasticity theory. The three curves LNE1, LNE2, and NIST are concave downward. Both of these laboratories use controlled-clearance piston gages as their primary standards. figure 20 implies that there is a fundamental disagreement between calculational or similarity methods and the controlled-clearance method.

All of the methods depend upon assumptions that are open to question. The controlled-clearance technique utilizes an auxiliary pressure on the outside of the cylinder to control the clearance between the piston and the cylinder. It is assumed that the auxiliary pressure is a linear function of the cube root of the rate at which the piston falls into the cylinder while the gage is operating for all loads on the piston. It is necessary also to extrapolate out of the range of these fall-rate measurements to obtain values used in the cylinder distortion term. The distance one must extrapolate is greatly influenced by the roundness of the piston and cylinder. In the derivation of the equation used in the calculation method, it is assumed that the pressure in the annulus is uniform when, in fact, there is a steep pressure gradient. It is also assumed that there are no shear stresses between planes passed through the cylinder normal to the cylindrical axis. The similarity method requires the radial separations between the pistons and cylinders at zero applied pressure be adjusted as

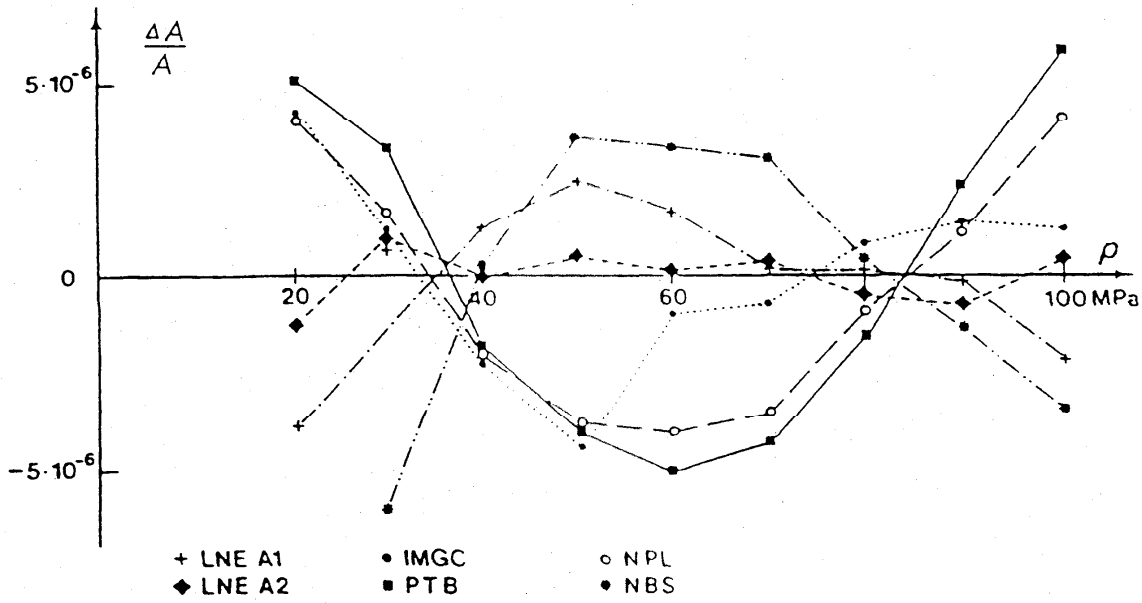


Figure 20. Residuals from fitting straight lines to the area data of the transfer standard provided by each laboratory and plotted as a function of pressure.

closely as possible to be in inverse ratio to the elastic moduli. Then it is assumed that as the pressure is increased, the pressure distribution between the pistons and cylinders of the two gages will be the same. Further research is needed to understand and reconcile the differences.

V. REFERENCES

- [1] L. A. Guildner, H. F. Stimson, R. E. Edsinger, and R. L. Anderson, *Metrologia* 6, 1 (1970).
- [2] L. A. Guildner and R. E. Edsinger, *J. Res. Natl. Bur. Stand. (U.S.)* 80A, 703 (1976).
- [3] J. F. Schooley, Proceedings of the 1988 Workshop and Symposium of the National Conference of Standards Laboratories, p. 50-1, August 14-18, 1988.
- [4] R. E. Edsinger, and J. F. Schooley, *Metrologia* 26, 95 (1989).
- [5] P.L.M. Heydemann and B. E. Welch in Experimental Thermodynamics, Volume II, edited by B. LeNeindre and B. Vodar (Butterworths, London, 1975), pp. 147-201.
- [6] D. R. Tate, *J. Res. Nat. Bur. Stand. (U.S.)* 72C (1968).
- [7] Handbook of Chemistry and Physics, F9 (52nd Edition), Chemical Rubber Publishing Company, Cleveland, OH (1971).
- [8] Precision Measurement and Calibration, U.S. Nat. Bur. Stand. (U.S.) Handb. No. 77, Vol. III, Government Printing Office, Washington, DC (1961).
- [9] R. M. Schoonover, *J. Res. Nat. Bur. Stand. (U.S.)* 85, 341 (1980).
- [10] B. E. Welch and V. E. Bean, *Rev. Sci. Instrum.* 55, 1901 (1984).
- [11] D. P. Johnson, J. L. Cross, J. D. Hill and A. H. Bowman, *Industr. Engng. Chem.* 49, 2046 (1957).
- [12] B. E. Welch, R. E. Edsinger, V. E. Bean, and C. D. Ehrlich, Observations of Gas Species and Mode of Operation Effects on Effective Areas of Gas-Operated Piston Gages, in High Pressure Metrology, G. F. Molinar, ed., Bureau International des Poids et Mesures, Monographie 89/1, (1988), p. 81.

[13] J. C. Legras, V. Bean, J. Jager, S. L. Lewis, G. F. Molinar, *J. Phys. E. Sci. Instrum.*, 18, 361 (1985).

[14] W. Markus, *Rev. Sci. Instrum.* 43, 158 (1972).

[15] J. C. Houck, G. F. Molinar, and R. Maghenzani, *J. Res. Nat. Bur. Stand. (U.S.)* 88 253 (1983).

[16] J. C. Lagras, S. L. Lewis, and G. F. Molinar, *Metrologia*, 25, 21, (1988).

[17] R. S. Dadson, in High Pressure Measurement Techniques, edited by G. N. Peggs (Applied Science Publishers, London, 1983), pp. 39-43.

VI. APPENDIX: SAMPLE CALIBRATION REPORT



NIST

UNITED STATES DEPARTMENT OF COMMERCE
National Institute of Standards and Technology
Gaithersburg, Maryland 20899-0001

P-0000A

Thermophics Division
A-55 Metrology Building

Requester:

Any One Testing
1234 Some Road N. E.
Pick-a-City, Pick-a-State 12345-1234

Test Instrument Data:

Manufacturer: X Y Z Instrument Corporation
Model: Pr 1111
Serial Number: Z111
Piston Number: Z111
Cylinder Number: ZC-Z000
Pressure Range: 1.38 MPa To 6.89 MPa
Cylinder Type: Simple
Thermal Expansion Coefficient of Piston: $4.55 \times 10^{-6} / ^\circ\text{C}$
Thermal Expansion Coefficient of Cylinder: $4.55 \times 10^{-6} / ^\circ\text{C}$
Nominal Piston Area: $1.39 \times 10^{-4} \text{ m}^2$

Test Record Data:

Purchase Order Number and Date: TP087654-43210 Dated 9/21/93
NIST Identification Number: P-0000A
NIST Test folder Number: TN-912543-93
Date Instrument was Received: November 31, 1993
Date Test was Completed: December 31, 1993

Test Conditions:

NIST Standard and Calibration Reference: PG 42, August 1988
Reference Temperature: 23°C
Pressure Fluid: Spinesso 22
Pressure Range of Calibration: 1.4 MPa To 6.9 MPa
Surface Tension of Fluid: 3.09E-2
Rotation of Weights: Manual
Test Gage Weights Provided by: NIST
The test gage was leveled so that the axis of rotation was vertical.
Reference level of test piston: The reference level is 0.073 meter below the uppermost surface of the piston. The gage was operated at mid-stroke.

The suggested fit for the effective area of the test gage is

$$\text{Area} = 1.422481 \times 10^{-4} * [1 + (-1.481 \times 10^{-12} * P)]$$

where P is the nominal pressure in Pa and the area is given in square meters.
The total uncertainty is 66 ppm based on the approximate triple standard deviation.

The test gage was cross-floated against the NIST standard. The calibration data are given in Table I. The pressures P are at the reference level of the test gage as determined by the NIST standard gage. The temperature corrected forces F on the test gage were calculated using the expression

$$F = \frac{\sum_i M_i (1 - \rho_a / \rho_m) g + \gamma C}{1 + (\alpha_p + \alpha_c)(T - 23)}$$

where M_i are the masses of the piston, weight hanger and weights corresponding to P,
 ρ_a is the density of the ambient air,
 ρ_m is the density of the material from which the weights are made,
 g is the local acceleration due to gravity,
 γ is the surface tension of the pressurizing fluid,
 C is the circumference of the piston in the test gage,
 α_p and α_c are the linear thermal expansivities of the piston and cylinder,
 and,
 T is the temperature in degrees C of the test gage when operating at pressure P.

Also listed in Table I is the area of the test gage at each pressure calculated using the expression

$$A = F/P$$

To obtain an expression for calculating the area at any pressure, the P and A data have been fitted to the following eight equations:

$$F = [A_0]P \quad (1)$$

$$F = [A_0]P - t \quad (2)$$

$$F = [A_0(1 + bP)] \quad (3)$$

$$F = [A_0(1 + bP)]P - t \quad (4)$$

$$F = [A_0(1 + bP + cP^2)]P \quad (5)$$

$$F = [A_0(1 + bP + cP^2)]P - t \quad (6)$$

$$F = [A_0(1 + cP^2)]P \quad (7)$$

$$F = [A_0(1 + cP^2)]P - t \quad (8)$$

where the term in brackets is the area as a function of pressure, A_0 is the extrapolated area at zero applied pressure and at 23 °C, b and c are the first and second order pressure coefficients for the area and t allows for the possibility of a tare. These coefficients and the tripled standard deviation associated with each coefficient are listed in Table III.

The test gage was cross-floated against the NIST standard. The calibration data are given in Table I. The pressures P are at the reference level of the test gage as determined by the NIST standard gage. The temperature corrected forces F on the test gage were calculated using the expression

$$F = \frac{\sum_i M_i (1 - \rho_a / \rho_m) g + \gamma C}{1 + (\alpha_p + \alpha_c)(T - 23)}$$

where M_i are the masses of the piston, weight hanger and weights corresponding to P,
 ρ_a is the density of the ambient air,
 ρ_m is the density of the material from which the weights are made,
 g is the local acceleration due to gravity,
 γ is the surface tension of the pressurizing fluid,
 C is the circumference of the piston in the test gage,
 α_p and α_c are the linear thermal expansivities of the piston and cylinder,
 and,
 T is the temperature in degrees C of the test gage when operating at pressure P.

Also listed in Table I is the area of the test gage at each pressure calculated using the expression

$$A = F/P$$

To obtain an expression for calculating the area at any pressure, the P and A data have been fitted to the following eight equations

$$A = A_0 \quad (1)$$

$$A = A_0 - t/P \quad (2)$$

$$A = A_0(1 + bP) \quad (3)$$

$$A = A_0(1 + bP) - t/P \quad (4)$$

$$A = A_0(1 + bP + cP^2) \quad (5)$$

$$A = A_0(1 + bP + cP^2) - t/P \quad (6)$$

$$A = A_0(1 + cP^2) \quad (7)$$

$$A = A_0(1 + cP^2) - t/P \quad (8)$$

where the term in brackets is the area as a function of pressure, A_0 is the extrapolated area at zero applied pressure and at 23 °C, b and c are the first and second order pressure coefficients for the area and t allows for the possibility of a tare. These coefficients and the tripled standard deviation associated with each coefficient are listed in Table III.

P-8465

TABLE I. CALIBRATION DATA

OBS. NO.	P PRESSURE (MPa)	F FORCE ON TEST GAGE (N)	F/P EXP. AREA (m ²)
1.0	1.427626E+00	2.03077E+02	1.422485E-04
2.0	1.427626E+00	2.03077E+02	1.422485E-04
3.0	2.805465E+00	3.990692E+02	1.422471E-04
4.0	4.872209E+00	6.930563E+02	1.422468E-04
5.0	6.939003E+00	9.870519E+02	1.422469E-04
6.0	6.939003E+00	9.870519E+02	1.422469E-04
7.0	6.250043E+00	8.890501E+02	1.422470E-04
8.0	4.183310E+00	5.950625E+02	1.422468E-04
9.0	4.183310E+00	5.950622E+02	1.422467E-04
10.0	2.116515E+00	3.010678E+02	1.422470E-04
9.0	7.629016E+01	1.281849E+03	1.680228E-05
10.0	3.493786E+01	5.870947E+02	1.680397E-05

TABLE II. COEFFICIENTS AND TRIPLED STANDARD DEVIATION OF THE COEFFICIENTS FROM FITS ACCORDING TO FORCE

FIT NO.	A ₀ ± ΔA ₀ , m ²	b ± Δb, (Pa) ⁻¹	c ± Δc, (Pa) ⁻²	t ± Δt, N
1	1.422470E-04	0.000000E+00	0.000000E+00	0.000000E+00
	2.415865E-10	0.000000E+00	0.000000E+00	0.000000E+00
2	1.422466E-04	0.000000E+00	0.000000E+00	-1.556432E-03
	4.535476E-10	0.000000E+00	0.000000E+00	2.081027E-03
3	1.422472E-04	-2.721360E-13	0.000000E+00	0.000000E+00
	1.007865E-09	1.192742E-12	0.000000E+00	0.000000E+00
4	1.422447E-04	1.635692E-12	0.000000E+00	-4.680329E-03
	1.397966E-09	1.152939E-12	0.000000E+00	2.495582E-03
5	1.422488E-04	-5.644814E-12	5.434030E-19	0.000000E+00
	1.880300E-09	5.639562E-12	5.637140E-19	0.000000E+00
6	1.422407E-04	9.370780E-12	-6.158568E-19	-8.718216E-03
	5.103034E-09	9.613867E-12	7.621957E-19	5.352064E-03
7	1.422470E-04	0.000000E+00	-1.422632E-20	0.000000E+00
	6.618505E-10	0.000000E+00	1.217329E-19	0.000000E+00
8	1.422456E-04	0.000000E+00	1.239066E-19	-3.716186E-03
	8.983719E-10	0.000000E+00	1.011768E-19	2.190966E-03

P-8465

TABLE III. COEFFICIENTS AND TRIPLED STANDARD DEVIATION OF THE COEFFICIENTS FROM FITS ACCORDING TO AREA

FIT NO.	$A_0 \pm \Delta A_0, m^2$	$b \pm \Delta b, (Pa)^{-1}$	$c \pm \Delta c, (Pa)^{-2}$	$+ \Delta t, N$
1	1.422472E-04 6.563554E-10	0.000000E+00 0.000000E+00	0.000000E+00 0.000000E+00	0.000000E+00 0.000000E+00
2	1.422463E-04 6.179310E-10	0.000000E+00 0.000000E+00	0.000000E+00 0.000000E+00	-2.819330E-03 1.566954E-03
3	1.422481E-04 1.192298E-09	-1.481821E-12 1.826769E-12	0.000000E+00 0.000000E+00	0.000000E+00 0.000000E+00
4	1.422441E-04 1.662107E-09	2.194630E-12 1.597867E-12	0.000000E+00 0.000000E+00	-5.631232E-03 2.238437E-03
5	1.422498E-04 1.612764E-09	-8.910301E-12 6.351027E-12	8.864457E-19 7.450572E-19	0.000000E+00 0.000000E+00
6	1.422401E-04 5.268654E-09	1.058918E-11 1.083068E-11	-7.183443E-19 9.206452E-19	-9.268421E-03 4.978454E-03
7	1.422477E-04 9.297143E-10	0.000000E+00 0.000000E+00	-1.411765E-19 2.397935E-19	0.000000E+00 0.000000E+00
8	1.422452E-04 1.049333E-09	0.000000E+00 0.000000E+00	1.757731E-19 1.531932E-19	-4.561128E-03 1.829370E-03

P-0000A

The suggested fit based on the calibration data is fit 3, yielding for the effective area

$$\text{Area} = A_0 [1 + (b_1 P)]$$

where P is the nominal pressure in Pa and the area is in square meters, chosen from the area fit.

The random uncertainty due to the calibration process can be expressed as the tripled approximate standard deviation of the predicted values of the area is 6.4 ppm. A measure of the total uncertainty of the area is then obtained by adding this value to the three sigma estimated systematic uncertainty of the NIST standard used which is 60 ppm. Thus, the total uncertainty of the effective area is 66 ppm. Note that this uncertainty is applicable only over the stated range of calibration, and furthermore is valid only for the specific operating conditions of this calibration, given on page 1.

NOTE: The mass used for the piston assembly was .0838687 kg, based on a density of 15.40 g/cm³, as reported by X Y Z Instrument Corp.

For the Director,
National Institute of Standards
and Technology

Charles D. Ehrlich, Physicist
Group Leader, Pressure Group
Thermophysics Division
Center for Chemical Technology

Values of characteristic parameters of the instrument are given in the following table(s).

To facilitate the detection of errors the weight numbers, gage temperatures, direction of rotation (1.=CW, -1.=CCW) and jacket pressure P_j are listed for all observations. Observation numbers 101 to 199 refer to the standard and 201 to 299 refer to the test instrument. Mass and density of the weights are listed in the PROGRAM weight table on pages 3 and 3(a).

OBS. NO.	TEMP °C	ROT	P_j (Pa)	WEIGHT NUMBERS					
101.	22.34	1.	0.	600.	601.	602.			
102.	22.34	1.	0.	600.	601.	602.			
103.	22.37	1.	0.	600.	601.	602.	92.		
104.	22.39	1.	0.	600.	601.	602.	92.	93.	
				105.					
105.	22.41	1.	0.	600.	601.	602.	92.	93.	
				94.	95.				
106.	22.41	1.	0.	600.	601.	602.	92.	93.	
				94.	95.				
107.	22.43	-1.	0.	600.	601.	602.	92.	93.	
				94.	105.				
108.	22.39	-1.	0.	600.	601.	602.	92.	93.	
109.	22.39	-1.	0.	600.	601.	602.	92.	93.	
110.	22.40	-1.	0.	600.	601.	602.	105.		
201.	22.50	1.	0.	603.	604.	605.	606.	607.	
				608.	609.	627.	630.	632.	
				464.	469.	471.	475.		
202.	22.50	-1.	0.	603.	604.	605.	606.	607.	
				608.	609.	627.	630.	632.	
				464.	469.	471.	475.		
203.	22.51	1.	0.	603.	604.	605.	606.	607.	
				608.	609.	610.	611.	612.	
				613.	627.	630.	464.	469.	
				473.	474.	475.	476.	632.	
204.	22.51	-1.	0.	603.	604.	605.	606.	607.	
				608.	609.	610.	611.	612.	
				613.	614.	615.	616.	617.	
				618.	619.	627.	630.	464.	
				470.	474.	477.	632.		
205.	22.51	1.	0.	603.	604.	605.	606.	607.	
				608.	609.	610.	611.	612.	
				613.	614.	615.	616.	617.	
				618.	619.	620.	621.	622.	
				623.	624.	625.	627.	630.	
				632.	464.	470.	473.	477.	
206.	22.51	-1.	0.	603.	604.	605.	606.	607.	
				608.	609.	610.	611.	612.	
				613.	614.	615.	616.	617.	
				618.	619.	620.	621.	622.	
				623.	624.	625.	627.	630.	
				632.	464.	470.	473.	477.	

PAGE 2 [cont'd]

207.	22.53	1.	0.	603.	604.	605.	606.	607.
				608.	609.	610.	611.	612.
				613.	614.	615.	616.	617.
				618.	619.	620.	621.	622.
				626.	627.	628.	631.	632.
				461.	466.	468.	470.	472.
208.	22.48	1.	0.	603.	604.	605.	606.	607.
				608.	609.	610.	611.	612.
				613.	614.	615.	616.	617.
				627.	630.	632.	464.	469.
				476.				
209.	22.48	-1.	0.	603.	604.	605.	606.	607.
				608.	609.	610.	611.	612.
				613.	614.	615.	616.	617.
				627.	630.	632.	464.	469.
				477.				
210.	22.48	-1.	0.	603.	604.	605.	606.	607.
				608.	609.	610.	611.	627.
				630.	632.	464.	469.	476.

Weights not listed in the Program Weight Table are assigned numbers: 600 to 699. Those used in this run ARE listed on this page. They include piston, weight hangers etc. of the instrument under test.

NUMBER	MASS (kg)	DENSITY (g/cm ³)
600.	0.083868700	15.400
601.	0.344963100	7.800
602.	11.799716000	7.800
603.	0.081155340	8.400
604.	0.174999565	8.400
605.	1.013779200	7.800
606.	0.804402000	7.800
607.	4.999401500	7.800
608.	5.000245000	7.800
609.	5.000281000	7.800
610.	5.000102000	7.800
611.	5.000275000	7.800
612.	4.999945000	7.800
613.	5.000188000	7.800
614.	5.000035000	7.800
615.	5.000232000	7.800
616.	5.000163000	7.800
617.	5.000203000	7.800
618.	5.000297000	7.800
619.	5.000316000	7.800
620.	5.000114000	7.800
621.	4.999980000	7.800
622.	5.000261000	7.800
623.	5.000019000	7.800
624.	5.000220000	7.800
625.	5.000194000	7.800
626.	3.000027000	7.800
627.	3.000075000	7.800
628.	2.000027000	7.800
629.	0.999983000	7.800
630.	0.500019700	7.800
631.	0.300001000	7.800
632.	0.099997800	8.400

Listed are the characteristics of the standard used in this test and available data for the instrument under test.

CHARACTERISTICS OF THE STANDARD

1.4200000E+02	Standard
8.4021380E-05	Area in m^2
-2.4000000E-12	Pressure Coefficient b_1 in Pa^{-1}
0.0000000E+00	Pressure Coefficient b_2 in Pa^{-2}
0.0000000E+00	
3.2480000E-02	Circumference of Piston in m
0.0000000E+00	Oil Buoyancy (volume in m^3) Correction Above Cylinder
4.1100000E-06	Thermal Expansivity of Piston $^{\circ}C^{-1}$
4.1100000E-06	Thermal Expansivity of Cylinder $^{\circ}C^{-1}$
0.0000000E+00	
2.3000000E+01	Reference Temperature of Standard $^{\circ}C$
0.0000000E+00	P_2 (Pa)
0.0000000E+00	S_2 ($Pa N^{-2}$) Zero Clearance Jacket Pressure (Coeff)
0.0000000E+00	Q_2 ($Pa N^{-1}$)
0.0000000E+00	D (Pa^{-1})
0.0000000E+00	E ($Pa^{-1} N^{-1}$) Jacket Pressure Distortion (Coeff)
0.0000000E+00	F ($Pa^{-1} N^{-2}$)
0.0000000E+00	
8.6000000E-05	3 Sigma A/A
2.4000000E-12	3 Sigma b_1
0.0000000E+00	3 Sigma b_2

CHARACTERISTICS OF INSTRUMENT UNDER TEST

2.0000000E+02	Instrument Under Test
1.4200000E-04	Area in m^2
0.0000000E+00	Pressure Coefficient b From Previous Calibration in Pa^{-1}
0.0000000E+00	
0.0000000E+00	
4.2400000E-02	Circumference of Piston in m
0.0000000E+00	Oil Buoyancy (volume in m^3)
4.5500000E-06	Thermal Expansivity of Piston $^{\circ}C^{-1}$
4.5500000E-06	Thermal Expansivity of Cylinder $^{\circ}C^{-1}$
-1.6300000E-01	Difference in Reference Levels in m
2.3000000E+01	Reference Temperature of the Instrument Under Test
8.5780000E-01	Density of Pressure Fluid in g/cm^3
0.0000000E+00	Pressure Coefficient of Density in Pa^{-1}
3.0930000E-02	Surface Tension of Pressure Fluid in $N m^{-1}$

Masses listed in the Program Weight Table are assigned numbers 001 to 599, and 701 to 2000.

Those used in this calibration are listed on this page.

* File 6tab81.tab MASS TABLE VALUES AS OF 09/91

Air Density used 0.00118 g/cm^3 Local Gravity is 9.801010 m/s^2

NUMBER	MASS kg	DENSITY g/cm^3
92.	.118133230E+02	0.840E+01
93.	.118132960E+02	0.840E+01
94.	.118130970E+02	0.840E+01
95.	.118132870E+02	0.840E+01
105.	.590641670E+01	0.840E+01
461.	.226798910E+00	0.780E+01
464.	.453600990E-01	0.780E+01
466.	.136078170E-01	0.780E+01
468.	.453596910E-02	0.780E+01
469.	.226802130E-02	0.780E+01
470.	.136066550E-02	0.780E+01
471.	.907253680E-03	0.780E+01
472.	.453621850E-03	0.166E+02
473.	.226796410E-03	0.166E+02
474.	.136055750E-03	0.166E+02
475.	.907930890E-04	0.166E+02
476.	.454732690E-04	0.166E+02
477.	.227166310E-04	0.270E+01

This table lists the force generated by the load on the standard instrument. An air buoyancy correction has been applied. Also listed are the corrections for surface tension, temperature, jacket pressure and pressure coefficient of the standard.

NO.	FORCE STD (N)	SURFACE TENS. (N)	TEMPERATURE CORR. STD	JACKET PRESSURE	PRESS. COEFF.	FRACTIONAL CHANGE (d)
101.	1.19834E+02	1.00461E-03	9.99995E-01	1.00000E+00	9.99997E-01	0.00000E+00
102.	1.19834E+02	1.00461E-03	9.99995E-01	1.00000E+00	9.99997E-01	0.00000E+00
103.	2.35600E+02	1.00461E-03	9.99995E-01	1.00000E+00	9.99993E-01	0.00000E+00
104.	4.09247E+02	1.00461E-03	9.99995E-01	1.00000E+00	9.99988E-01	0.00000E+00
105.	5.82896E+02	1.00461E-03	9.99995E-01	1.00000E+00	9.99983E-01	0.00000E+00
106.	5.82896E+02	1.00461E-03	9.99995E-01	1.00000E+00	9.99983E-01	0.00000E+00
107.	5.25011E+02	1.00461E-03	9.99995E-01	1.00000E+00	9.99985E-01	0.00000E+00
108.	3.51366E+02	1.00461E-03	9.99995E-01	1.00000E+00	9.99990E-01	0.00000E+00
109.	3.51366E+02	1.00461E-03	9.99995E-01	1.00000E+00	9.99990E-01	0.00000E+00
110.	1.77715E+02	1.00461E-03	9.99995E-01	1.00000E+00	9.99995E-01	0.00000E+00

This table lists the force generated by the load on the instrument under test. An air buoyancy correction has been applied. Also listed are the corrections for surface tension, temperature and fluid head in the connecting lines between the two instruments.

NO.	FORCE TEST (N)	FLUID BUOY. TEST (N)	SURFACE TENS. (N)	TEMP. CORR. TEST	HEAD CORR. (Pa)
201.	0.2030754E+03	0.0000000E+00	0.1311432E-02	0.9999955E+00	-0.1368504E+04
202.	0.2030754E+03	0.0000000E+00	0.1311432E-02	0.9999955E+00	-0.1368504E+04
203.	0.3990661E+03	0.0000000E+00	0.1311432E-02	0.9999955E+00	-0.1368504E+04
204.	0.6930518E+03	0.0000000E+00	0.1311432E-02	0.9999955E+00	-0.1368504E+04
205.	0.9870462E+03	0.0000000E+00	0.1311432E-02	0.9999955E+00	-0.1368504E+04
206.	0.9870462E+03	0.0000000E+00	0.1311432E-02	0.9999955E+00	-0.1368504E+04
207.	0.8890450E+03	0.0000000E+00	0.1311432E-02	0.9999957E+00	-0.1368504E+04
208.	0.5950584E+03	0.0000000E+00	0.1311432E-02	0.9999953E+00	-0.1368504E+04
209.	0.5950581E+03	0.0000000E+00	0.1311432E-02	0.9999953E+00	-0.1368504E+04
210.	0.3010651E+03	0.0000000E+00	0.1311432E-02	0.9999953E+00	-0.1368504E+04

After computation of the pressure generated by the standard at the reference level of the instrument under test, the following functions are fitted to the data.

FORCE EQUATIONS

- | | |
|--------------------------------|--|
| FIT 1 $F=PA_0$ | FIT 5 $F=PA_0 [1+(b_1 P)+(b_2 P^2)]$ |
| FIT 2 $F=PA_0 - t$ | FIT 6 $F=PA_0 [1+(b_1 P)+(b_2 P^2)] - t$ |
| FIT 3 $F=PA_0 [1+(b_1 P)]$ | FIT 7 $F=PA_0 [1+(b_2 P^2)]$ |
| FIT 4 $F=PA_0 [1+(b_1 P)] - t$ | FIT 8 $F=PA_0 [1+(b_2 P^2)] - t$ |

With: F Force on test instrument
 P Pressure at Ref Level
 A_0 Effective Area of test instrument at Zero pressure
 b_1 and b_2 Pressure Coefficients
 t Tare Weight (force).

This table lists the observation numbers, pressure and the residuals of the fits converted to the equivalent pressures.

OBS. NO.	PRESSURE kPa	RESIDUALS FIT 1, Pa	RESIDUALS FIT 2, Pa	RESIDUALS FIT 3, Pa	RESIDUALS FIT 4, Pa
0.	0.000000E+00	0.000000E+00	-0.10942E+02	0.000000E+00	-0.32903E+02
1.	0.142763E+04	0.15982E+02	0.80931E+01	0.14300E+02	0.23669E+01
2.	0.142763E+04	0.15982E+02	0.80931E+01	0.14300E+02	0.23669E+01
10.	0.211651E+04	-0.61656E-01	-0.64775E+01	-0.21580E+01	-0.67546E+01
3.	0.280547E+04	0.21611E+01	-0.27815E+01	-0.91617E-01	0.83833E+00
8.	0.418331E+04	-0.44270E+01	-0.64232E+01	-0.62175E+01	0.33221E+00
9.	0.418331E+04	-0.59954E+01	-0.79916E+01	-0.77859E+01	-0.12362E+01
4.	0.487221E+04	-0.47538E+01	-0.52769E+01	-0.59258E+01	0.71743E+00
7.	0.625004E+04	0.36083E+01	0.60315E+01	0.44484E+01	0.58459E+01
5.	0.693900E+04	-0.53004E+00	0.33665E+01	0.17036E+01	-0.22384E+01
6.	0.693900E+04	-0.53004E+00	0.33665E+01	0.17036E+01	-0.22384E+01

OBS. NO.	PRESSURE kPa	RESIDUALS FIT 5, Pa	RESIDUALS FIT 6, Pa	RESIDUALS FIT 7, Pa	RESIDUALS FIT 8, Pa
0.	0.000000E+00	0.000000E+00	-0.612893E+02	0.000000E+00	-0.261249E+02
1.	0.142763E+04	0.689423E+01	0.464599E+00	0.153068E+02	0.302773E+01
2.	0.142763E+04	0.689423E+01	0.464599E+00	0.153068E+02	0.302773E+01
10.	0.211651E+04	-0.811235E+01	-0.397241E+01	-0.989297E+00	-0.730094E+01
3.	0.280547E+04	-0.276921E+01	0.467506E+01	0.106687E+01	-0.109428E+00
8.	0.418331E+04	-0.113204E+01	0.219682E+00	-0.548556E+01	0.267605E-01
9.	0.418331E+04	-0.270047E+01	-0.134875E+01	-0.705400E+01	-0.154167E+01
4.	0.487221E+04	0.151389E+01	-0.198239E+01	-0.555432E+01	0.969509E+00
7.	0.625004E+04	0.821196E+01	0.278647E+01	0.394397E+01	0.647049E+01
5.	0.693900E+04	-0.269595E+01	-0.653431E+00	0.739648E+00	-0.228509E+01
6.	0.693900E+04	-0.269595E+01	-0.653431E+00	0.739648E+00	-0.228509E+01

This table lists the observation numbers, pressure and the standard deviations of the predicted values, expressed in Parts Per Million (ppm).

OBS. NO.	PRESSURE KPA	3 SD PRED FIT 1, ppm	3 SD PRED FIT 2, ppm	3 SD PRED FIT 3, ppm	3 SD PRED FIT 4, ppm
0.	0.000000E+00	0.000000E+00	0.693676E-03	0.000000E+00	0.831861E-03
1.	0.142763E+04	0.169834E+01	0.752192E+01	0.545154E+01	0.510055E+01
2.	0.142763E+04	0.169834E+01	0.752192E+01	0.545154E+01	0.510055E+01
10.	0.211651E+04	0.169836E+01	0.429170E+01	0.468090E+01	0.242395E+01
3.	0.280547E+04	0.169836E+01	0.274598E+01	0.393084E+01	0.179695E+01
8.	0.418331E+04	0.169836E+01	0.154878E+01	0.256607E+01	0.143516E+01
9.	0.418331E+04	0.169836E+01	0.154878E+01	0.256608E+01	0.143516E+01
4.	0.487221E+04	0.169836E+01	0.141854E+01	0.204377E+01	0.118026E+01
7.	0.625004E+04	0.169836E+01	0.150345E+01	0.184729E+01	0.848793E+00
5.	0.693900E+04	0.169836E+01	0.159854E+01	0.224855E+01	0.106683E+01
6.	0.693900E+04	0.169836E+01	0.159854E+01	0.224855E+01	0.106683E+01

OBS. NO.	PRESSURE KPA	3 SD PRED FIT 5, ppm	3 SD PRED FIT 6, ppm	3 SD PRED FIT 7, ppm	3 SD PRED FIT 8, ppm
0.	0.000000E+00	0.000000E+00	0.178402E-02	0.000000E+00	0.730322E-03
1.	0.142763E+04	0.666613E+01	0.424899E+01	0.442474E+01	0.552048E+01
2.	0.142763E+04	0.666613E+01	0.424899E+01	0.442474E+01	0.552048E+01
10.	0.211651E+04	0.446395E+01	0.247184E+01	0.415465E+01	0.269989E+01
3.	0.280547E+04	0.300438E+01	0.218358E+01	0.378619E+01	0.188354E+01
8.	0.418331E+04	0.224036E+01	0.110234E+01	0.280796E+01	0.158784E+01
9.	0.418331E+04	0.224036E+01	0.110234E+01	0.280796E+01	0.158784E+01
4.	0.487221E+04	0.216431E+01	0.113640E+01	0.227432E+01	0.137160E+01
7.	0.625004E+04	0.147214E+01	0.889763E+00	0.184583E+01	0.940994E+00
5.	0.693900E+04	0.175083E+01	0.866464E+00	0.237642E+01	0.119983E+01
6.	0.693900E+04	0.175083E+01	0.866464E+00	0.237642E+01	0.119983E+01

In order to detect any effect due to the rotational direction of the pistons, the residuals from FIT 6 are separated with respect to the direction of rotation of the pistons and tabulated.

OBS. NO.	PRESSURE kPa	1=CW -1=CCW	TEST CW, Pa	TEST CCW, Pa	1=CW -1=CCW	STD. CW, Pa	STD. CCW, Pa
0.	0.0000E+00	0.	0.0000E+00	0.0000E+00	0.	0.0000E+00	0.0000E+00
1.	0.1428E+04	1.	0.4646E+00	0.0000E+00	1.	0.4646E+00	0.0000E+00
2.	0.1428E+04	-1.	0.0000E+00	0.4646E+00	1.	0.4646E+00	0.0000E+00
10.	0.2117E+04	-1.	0.0000E+00	-.3972E+01	-1.	0.0000E+00	-.3972E+01
3.	0.2805E+04	1.	0.4675E+01	0.0000E+00	1.	0.4675E+01	0.0000E+00
8.	0.4183E+04	1.	0.2197E+00	0.0000E+00	-1.	0.0000E+00	0.2197E+00
9.	0.4183E+04	-1.	0.0000E+00	-.1349E+01	-1.	0.0000E+00	-.1349E+01
4.	0.4872E+04	-1.	0.0000E+00	-.1982E+01	1.	-.1982E+01	0.0000E+00
7.	0.6250E+04	1.	0.2786E+01	0.0000E+00	-1.	0.0000E+00	0.2786E+01
5.	0.6939E+04	1.	-.6534E+00	0.0000E+00	1.	-.6534E+00	0.0000E+00
6.	0.6939E+04	-1.	0.0000E+00	-.6534E+00	1.	-.6534E+00	0.0000E+00

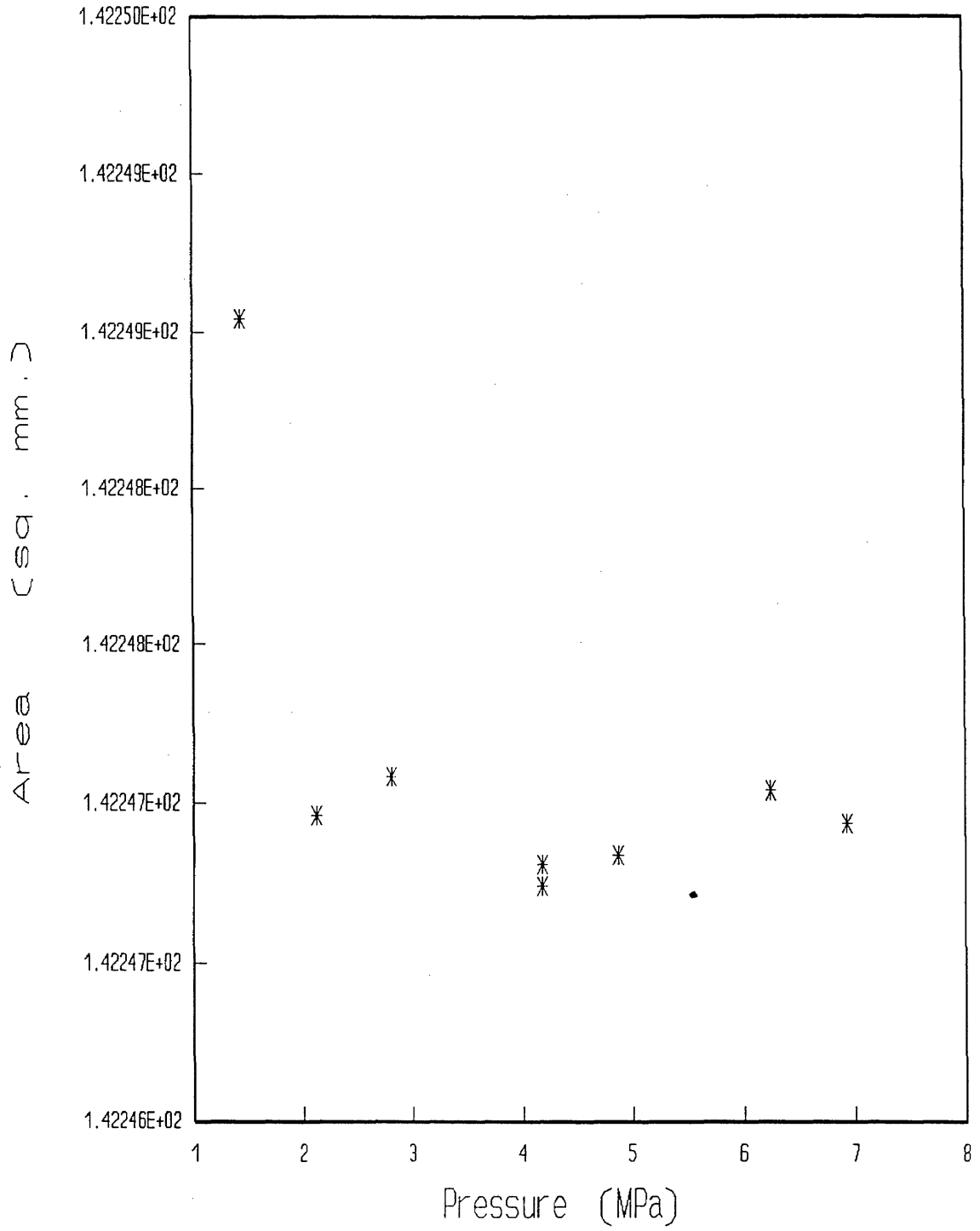
The results of the test, as determined by using the FORCE EQUATIONS, are compiled in this table. It lists the coefficients and their tripled standard deviations due to random sources of error and, for the highest pressure, the uncertainty in pressure due to the uncertainty in these coefficients.

COEFF, FIT 1	COEFF, FIT 2	COEFF, FIT 3	COEFF, FIT 4	
1.422470E-04	1.422466E-04	1.422472E-04	1.422447E-04	AREA, M ²
0.000000E+00	0.000000E+00	-2.721360E-13	1.635692E-12	PRES COEF b ₁ Pa ⁻¹
0.000000E+00	0.000000E+00	0.000000E+00	0.000000E+00	PRES COEF b ₂ Pa ⁻²
0.000000E+00	0.000000E+00	0.000000E+00	0.000000E+00	
0.000000E+00	-1.556432E-03	0.000000E+00	-4.680329E-03	TARE, N
1.698359E-06	3.188460E-06	7.085308E-06	9.827898E-06	3 STD DEV A ₀ /A ₀ ⁻¹
0.000000E+00	0.000000E+00	1.192742E-12	1.152939E-12	3 STD DEV b ₁ Pa ⁻²
0.000000E+00	0.000000E+00	0.000000E+00	0.000000E+00	3 STD DEV b ₂ Pa ⁻²
0.000000E+00	0.000000E+00	0.000000E+00	0.000000E+00	
0.000000E+00	2.081027E-03	0.000000E+00	2.495582E-03	3 STD DEV T, N
2.464246E-02	2.047674E-02	2.540394E-02	1.155705E-02	3 RES STD DEV kPa
1.698359E-06	5.296785E-06	1.536175E-05	2.035646E-05	3 STD DEV A _e /A _e at P _{max}
COEFF, FIT 5	COEFF, FIT 6	COEFF, FIT 7	COEFF, FIT 8	
1.422488E-04	1.422407E-04	1.422470E-04	1.422456E-04	AREA, M ²
-5.644814E-12	9.370780E-12	0.000000E+00	0.000000E+00	PRES COEF b ₁ Pa ⁻¹
5.434030E-19	-6.158568E-19	-1.422632E-20	1.239066E-19	PRES COEF b ₂ Pa ⁻²
0.000000E+00	0.000000E+00	0.000000E+00	0.000000E+00	
0.000000E+00	-8.718216E-03	0.000000E+00	-3.716186E-03	TARE, N
1.321839E-05	3.587605E-05	4.652826E-06	6.315639E-06	3 STD DEV A ₀ /A ₀ ⁻¹
5.639562E-12	9.613867E-12	0.000000E+00	0.000000E+00	3 STD DEV b ₁ Pa ⁻²
5.637140E-19	7.621957E-19	1.217329E-19	1.011768E-19	3 STD DEV b ₂ Pa ⁻²
0.000000E+00	0.000000E+00	0.000000E+00	0.000000E+00	
0.000000E+00	5.352064E-03	0.000000E+00	2.190966E-03	3 STD DEV T, N
1.833163E-02	8.873121E-03	2.593875E-02	1.279243E-02	3 RES STD DEV kPa
7.949402E-05	1.447085E-04	1.051424E-05	1.340698E-05	3 STD DEV A _e /A _e at P _{max}

P (Pa)	AREA, m ²	P (MPa)	AREA, mm ²
0.14276260E+07	0.14224854E-03	0.14276260E+01	0.14224854E+03
0.14276260E+07	0.14224854E-03	0.14276260E+01	0.14224854E+03
0.28054650E+07	0.14224708E-03	0.28054650E+01	0.14224708E+03
0.48722090E+07	0.14224684E-03	0.48722090E+01	0.14224684E+03
0.69390030E+07	0.14224694E-03	0.69390030E+01	0.14224694E+03
0.69390030E+07	0.14224694E-03	0.69390030E+01	0.14224694E+03
0.62500430E+07	0.14224704E-03	0.62500430E+01	0.14224704E+03
0.41833100E+07	0.14224681E-03	0.41833100E+01	0.14224681E+03
0.41833100E+07	0.14224674E-03	0.41833100E+01	0.14224674E+03
0.21165150E+07	0.14224696E-03	0.21165150E+01	0.14224696E+03

This data represents the effective area of the TEST GAGE, determined as the full air buoyancy corrected force on the test gage divided by the pressure at the reference level of the test gage. The equations on PAGE 10 are fit to this data.

Area vs Pressure (Data on Page 9)



After computation of the pressure generated by the standard at the reference level of the instrument under test the following functions are fitted to the data.

AREA EQUATIONS

FIT 1 $A=A_0$	FIT 5 $A=A_0 [1+(b_1 P)+(b_2 P^2)]$
FIT 2 $A=A_0 - (t/P)$	FIT 6 $A=A_0 [1+(b_1 P)+(b_2 P^2)] - (t/P)$
FIT 3 $A=A_0 [1+(b_1 P)]$	FIT 7 $A=A_0 [1+(b_2 P^2)]$
FIT 4 $A=A_0 [1+(b_1 P)] - (t/P)$	FIT 8 $A=A_0 [1+(b_2 P^2)] - (t/P)$

With: P Pressure at Ref Level
 A Effective Area of Test Instrument at each observation
 b_1 and b_2 Pressure Coefficients
 t Tare (force in newtons)

This table lists the observation numbers, pressure and the residuals of the fits converted to the equivalent pressures.

OBS. NO.	PRESSURE kPa	RESIDUALS FIT 1, Pa	RESIDUALS FIT 2, Pa	RESIDUALS FIT 3, Pa	RESIDUALS FIT 4, Pa
1.	0.142763E+04	0.130298E+02	0.272127E+01	0.734600E+01	0.857584E+00
2.	0.142763E+04	0.130298E+02	0.272127E+01	0.734600E+01	0.857584E+00
3.	0.280547E+04	-0.324452E+01	-0.437363E+01	-0.868611E+01	0.255919E+01
4.	0.487221E+04	-0.138593E+02	-0.121910E+01	-0.838813E+01	0.328502E+01
5.	0.693900E+04	-0.147186E+02	0.116912E+02	0.143251E+02	-0.498220E+01
6.	0.693900E+04	-0.147186E+02	0.116912E+02	0.143251E+02	-0.498220E+01
7.	0.625004E+04	-0.880864E+01	0.130111E+02	0.109705E+02	0.548043E+01
8.	0.418331E+04	-0.127313E+02	-0.468078E+01	-0.123042E+02	0.271600E+01
9.	0.418331E+04	-0.148403E+02	-0.678980E+01	-0.144132E+02	0.606976E+00
10.	0.211651E+04	-0.425524E+01	-0.997434E+01	-0.105213E+02	-0.639840E+01

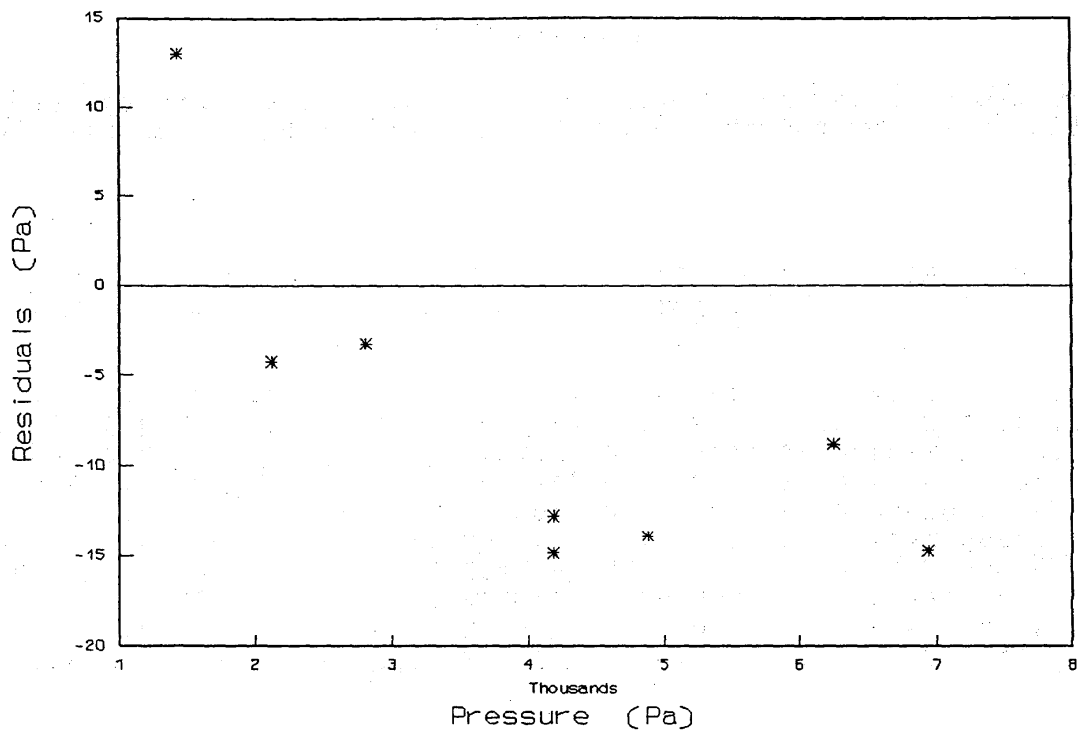
OBS. NO.	PRESSURE kPa	RESIDUALS FIT 5, Pa	RESIDUALS FIT 6, Pa	RESIDUALS FIT 7, Pa	RESIDUALS FIT 8, Pa
1.	0.142763E+04	0.291558E+01	0.256754E+00	0.919752E+01	0.112396E+01
2.	0.142763E+04	0.291558E+01	0.256754E+00	0.919752E+01	0.112396E+01
3.	0.280547E+04	-0.318241E+01	0.536278E+01	-0.846554E+01	0.142916E+01
4.	0.487221E+04	0.744012E+01	-0.200112E+01	-0.120120E+02	0.429009E+01
5.	0.693900E+04	-0.675284E+01	-0.373053E+00	0.118264E+02	-0.504226E+01
6.	0.693900E+04	-0.675284E+01	-0.373053E+00	0.118264E+02	-0.504226E+01
7.	0.625004E+04	0.103418E+02	0.244383E+01	0.708297E+01	0.670576E+01
8.	0.418331E+04	0.301154E+01	0.698928E-02	-0.148295E+02	0.290519E+01
9.	0.418331E+04	0.902523E+00	-0.210203E+01	-0.169385E+02	0.796166E+00
10.	0.211651E+04	-0.108392E+02	-0.347787E+01	-0.920735E+01	-0.734207E+01

This table lists the observation numbers, pressure and the standard deviations of the predicted values, expressed in Parts Per Million (ppm).

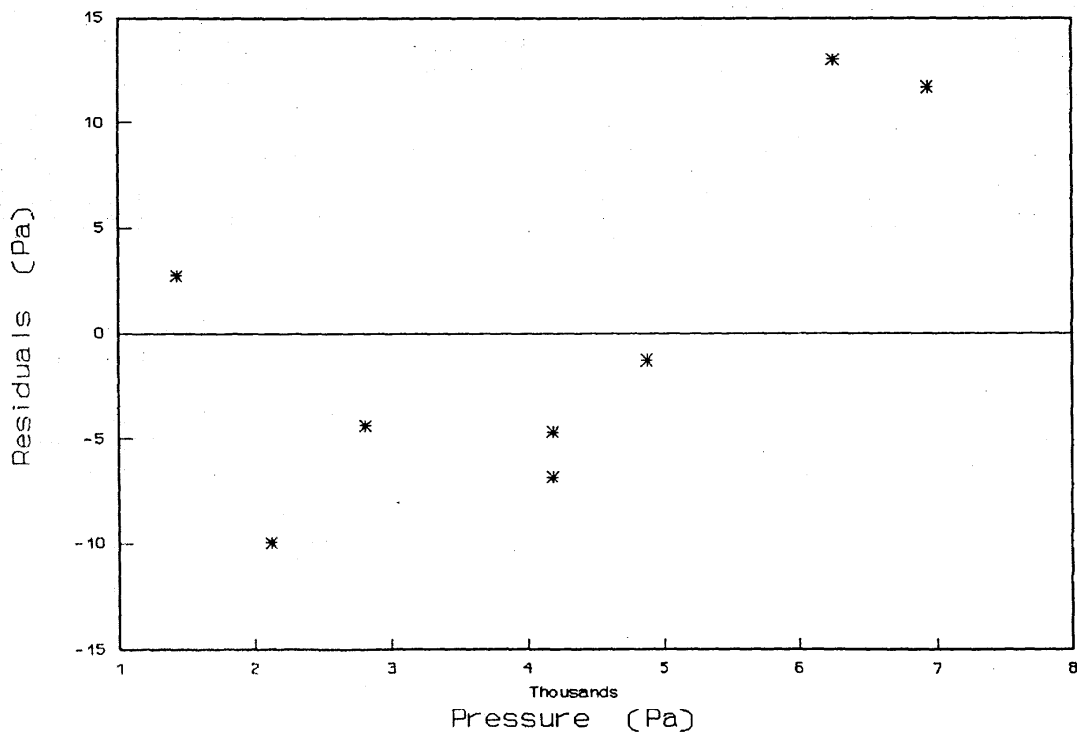
OBS. NO.	PRESSURE KPA	3 SD PRED FIT 1, ppm	3 SD PRED FIT 2, ppm	3 SD PRED FIT 3, ppm	3 SD PRED FIT 4, ppm
1.	0.142763E+04	0.461415E+01	0.461149E+01	0.615248E+01	0.282817E+01
2.	0.142763E+04	0.461415E+01	0.461149E+01	0.615248E+01	0.282817E+01
3.	0.280547E+04	0.461419E+01	0.228254E+01	0.441376E+01	0.223057E+01
4.	0.487221E+04	0.461420E+01	0.269055E+01	0.395981E+01	0.169360E+01
5.	0.693900E+04	0.461420E+01	0.310396E+01	0.635519E+01	0.250502E+01
6.	0.693900E+04	0.461420E+01	0.310396E+01	0.635519E+01	0.250502E+01
7.	0.625004E+04	0.461419E+01	0.298745E+01	0.538369E+01	0.193579E+01
8.	0.418331E+04	0.461420E+01	0.251077E+01	0.371208E+01	0.193922E+01
9.	0.418331E+04	0.461420E+01	0.251077E+01	0.371208E+01	0.193922E+01
10.	0.211651E+04	0.461420E+01	0.272312E+01	0.520424E+01	0.199682E+01

OBS. NO.	PRESSURE KPA	3 SD PRED FIT 5, ppm	3 SD PRED FIT 6, ppm	3 SD PRED FIT 7, ppm	3 SD PRED FIT 8, ppm
1.	0.142763E+04	0.470577E+01	0.227341E+01	0.616617E+01	0.315861E+01
2.	0.142763E+04	0.470577E+01	0.227341E+01	0.616617E+01	0.315861E+01
3.	0.280547E+04	0.325791E+01	0.216203E+01	0.521770E+01	0.233687E+01
4.	0.487221E+04	0.371623E+01	0.191900E+01	0.420086E+01	0.201089E+01
5.	0.693900E+04	0.478399E+01	0.213336E+01	0.771056E+01	0.291659E+01
6.	0.693900E+04	0.478399E+01	0.213336E+01	0.771056E+01	0.291659E+01
7.	0.625004E+04	0.342834E+01	0.163487E+01	0.599034E+01	0.213567E+01
8.	0.418331E+04	0.387989E+01	0.172684E+01	0.423772E+01	0.227451E+01
9.	0.418331E+04	0.387990E+01	0.172684E+01	0.423772E+01	0.227451E+01
10.	0.211651E+04	0.331547E+01	0.235774E+01	0.574685E+01	0.207900E+01

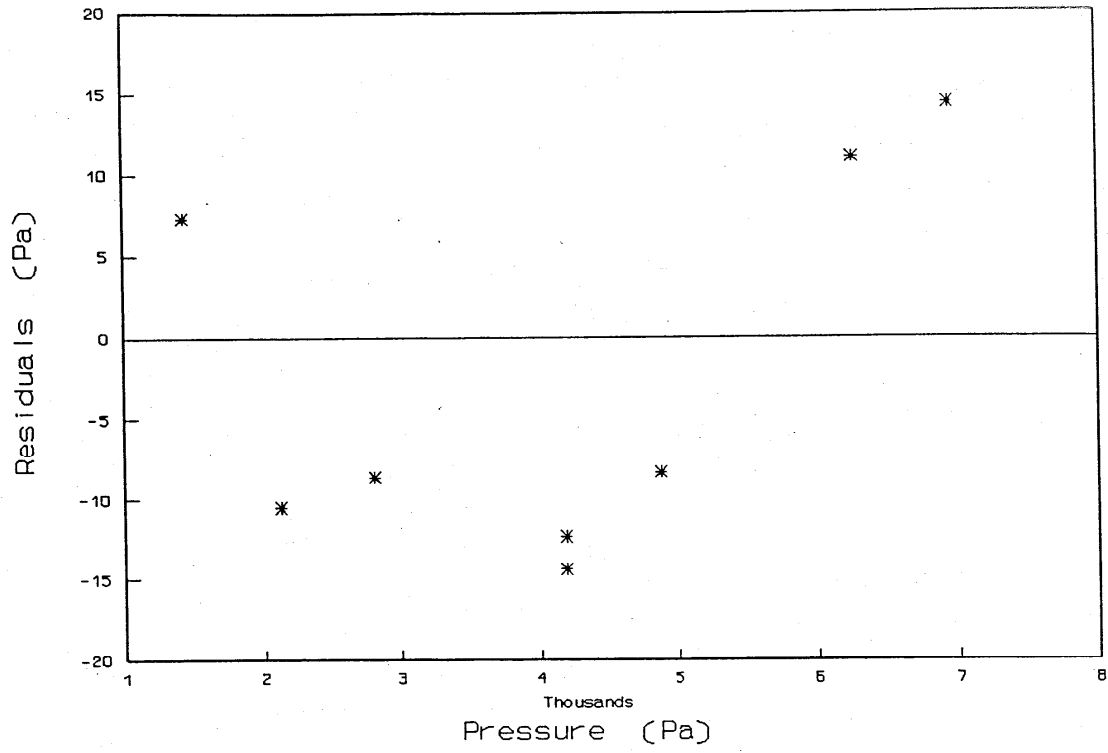
Residuals of Fit 1



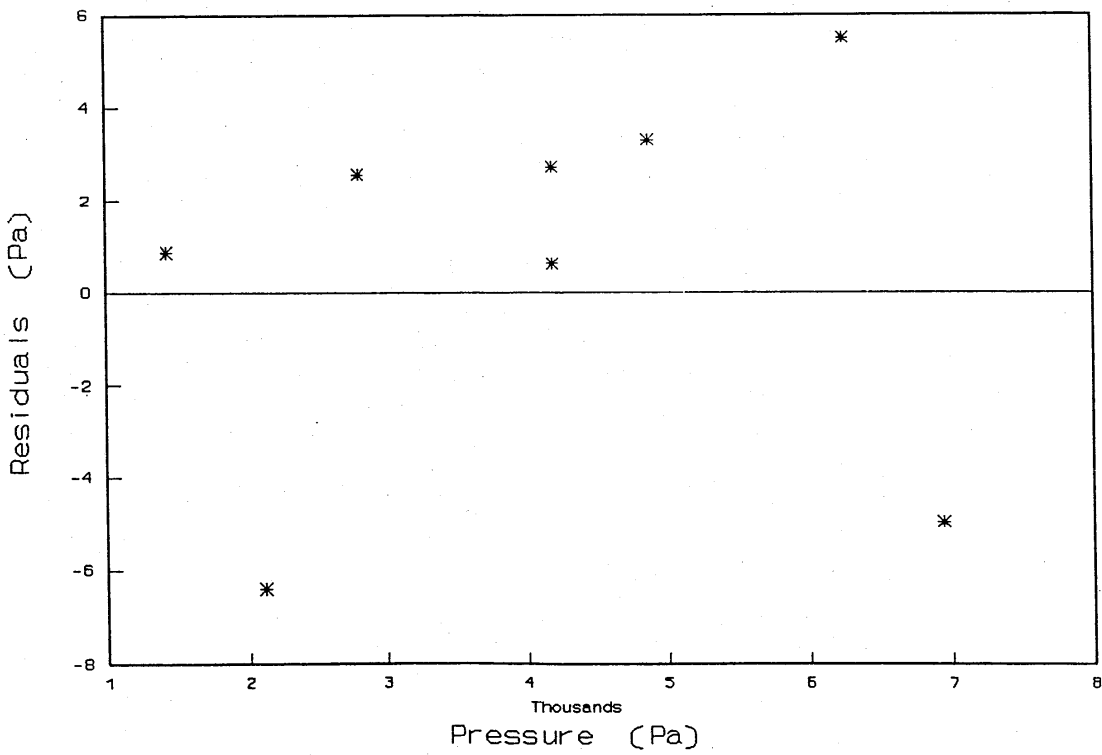
Residuals of Fit 2



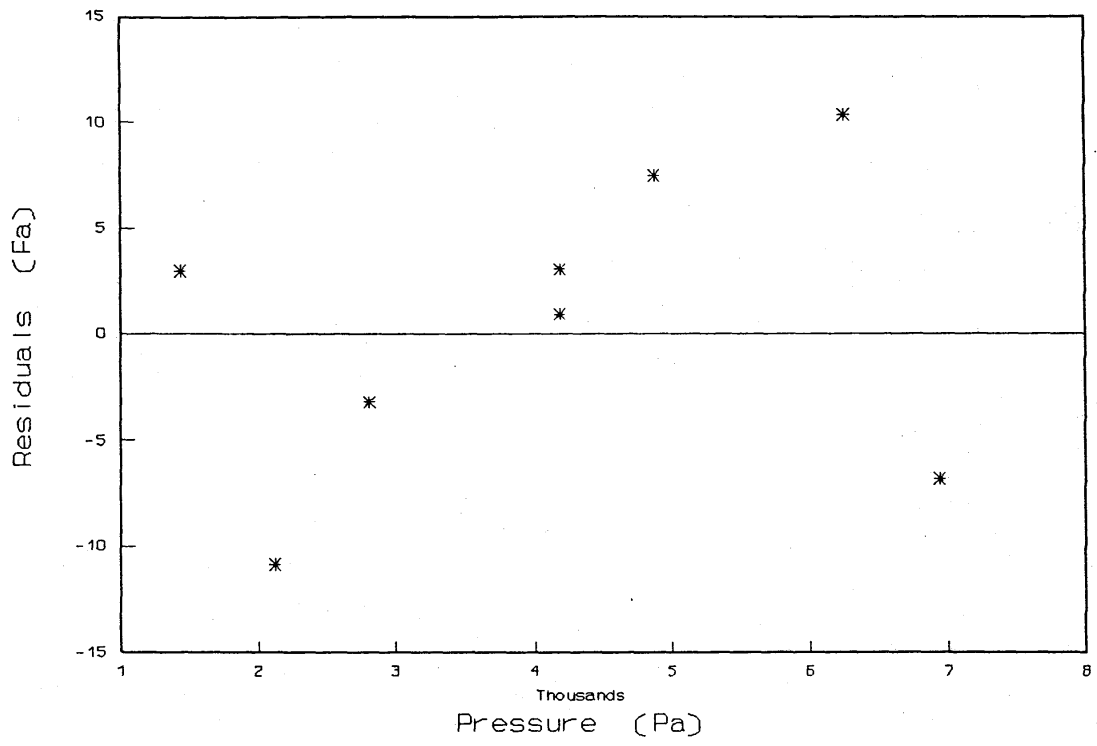
Residuals of Fit 3



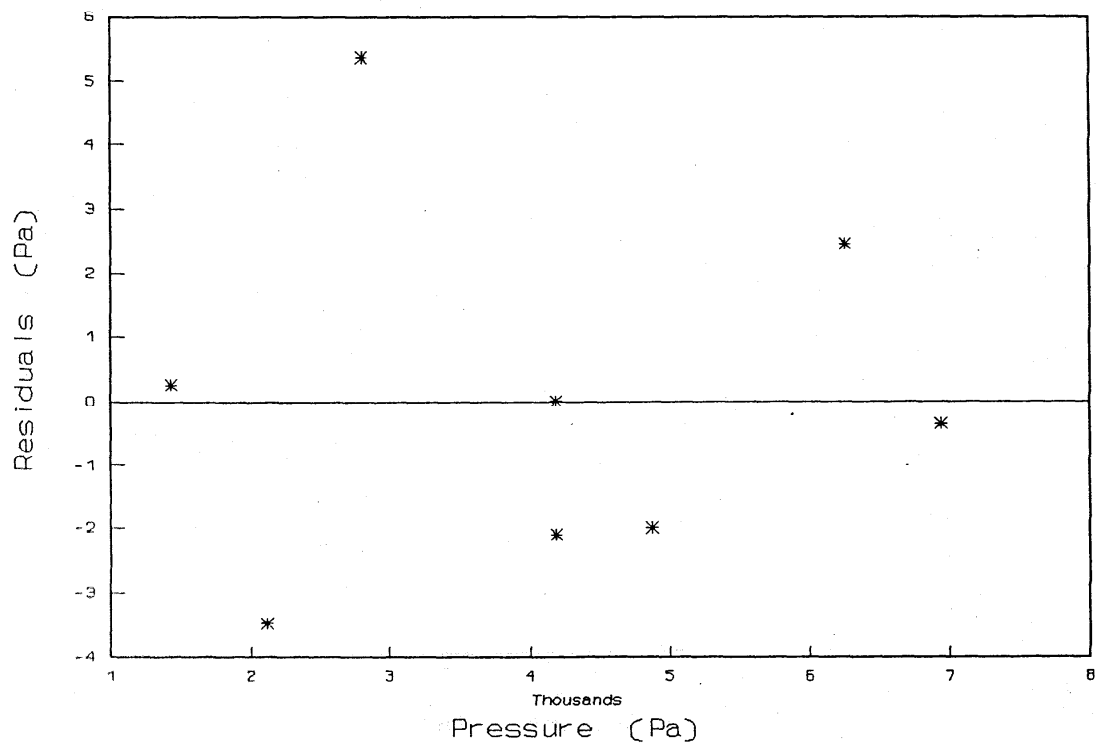
Residuals of Fit 4



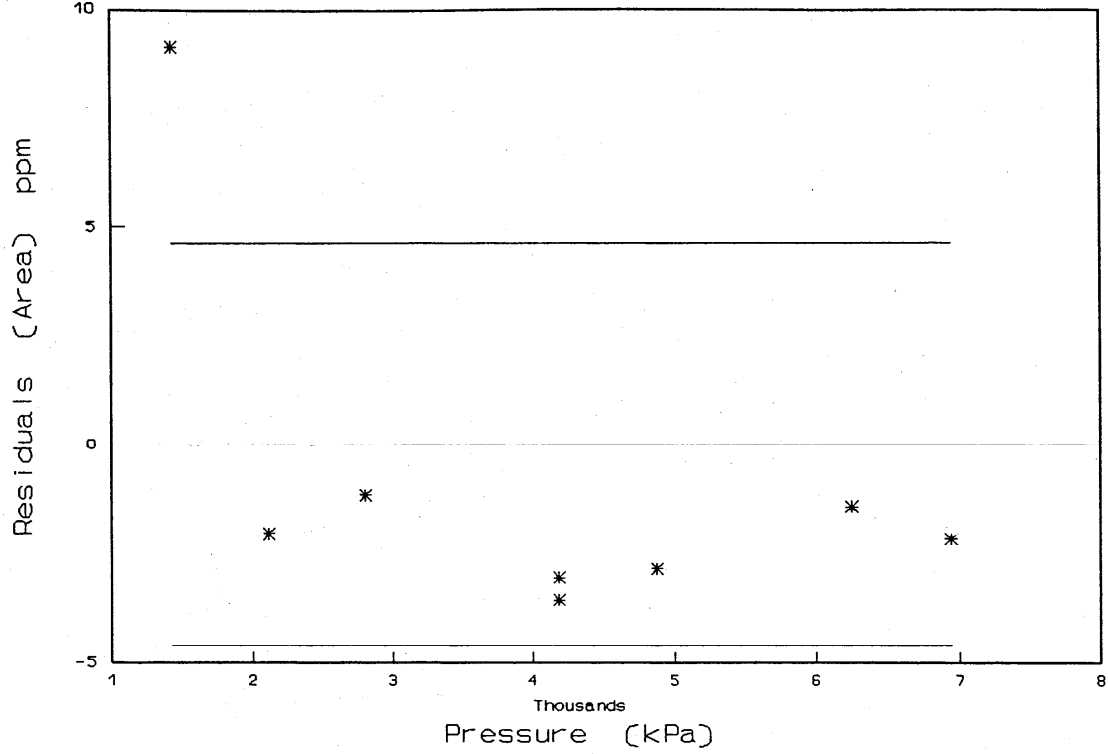
Residuals of Fit 5



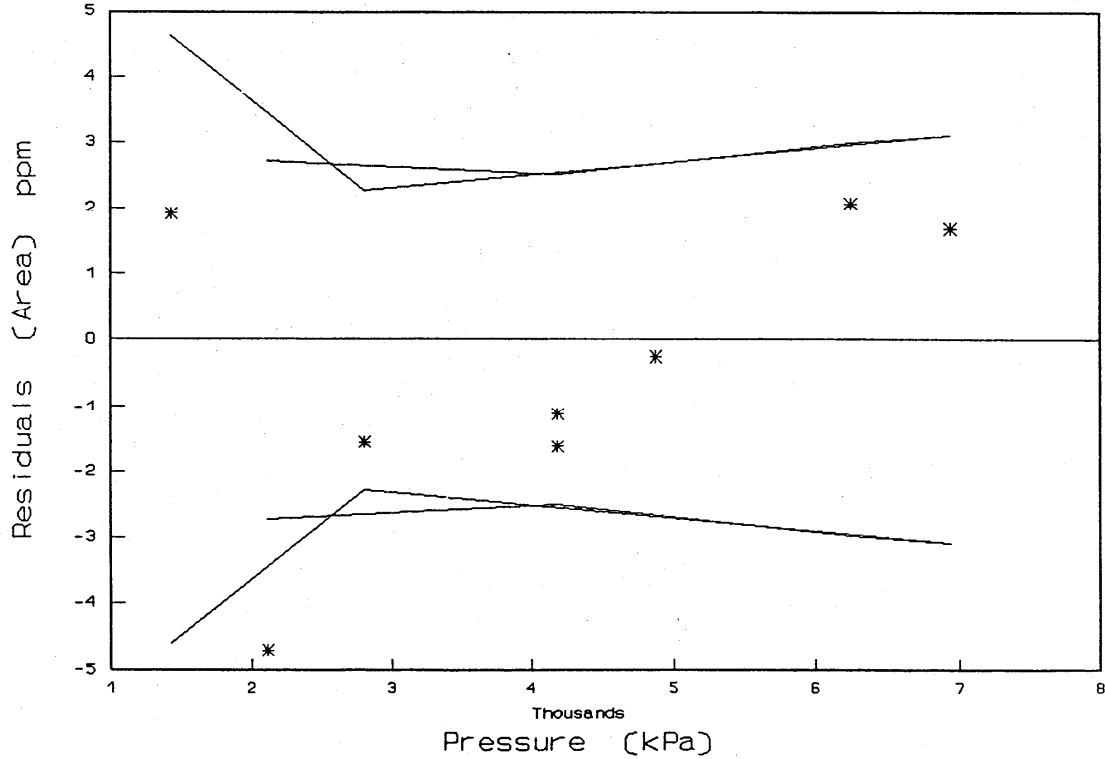
Residuals of Fit 6



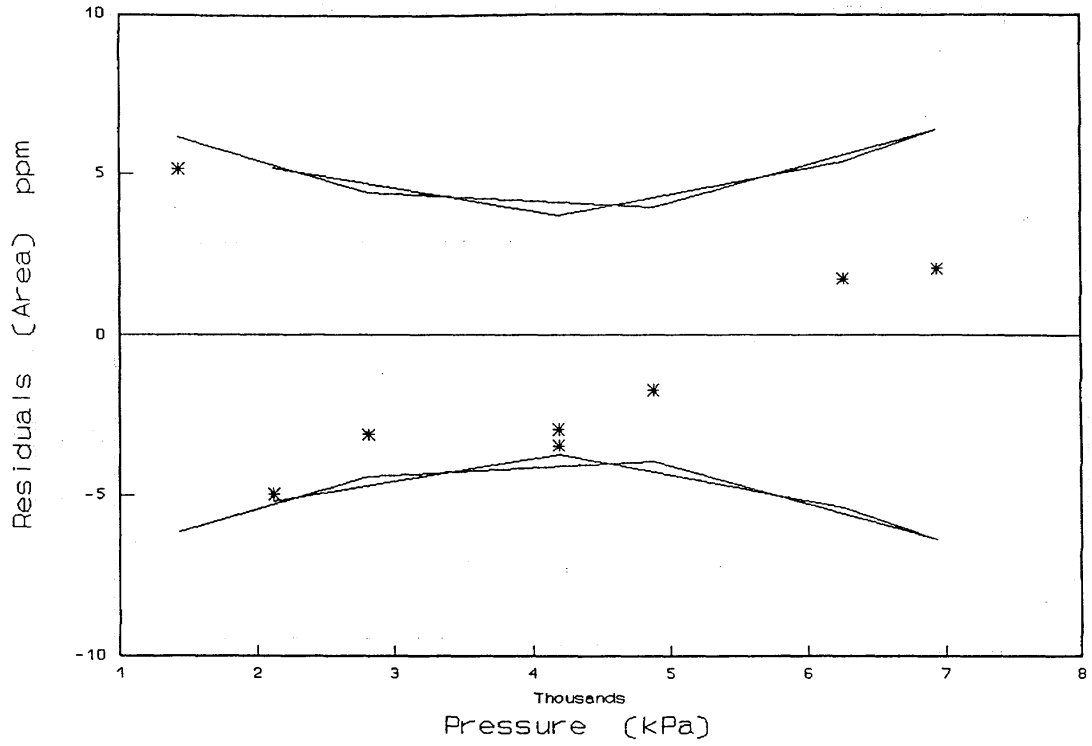
Residuals in ppm (3 Sigma Error Bars Applied) Fit 1



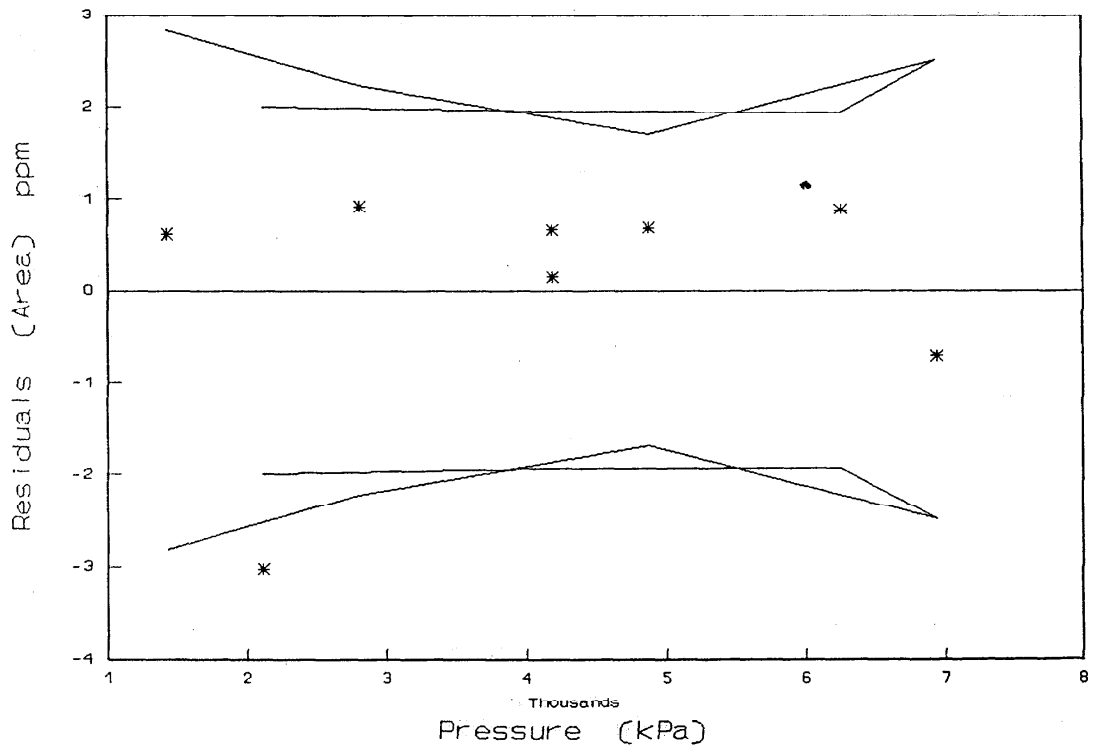
Residuals in ppm (3 Sigma Error Bars Applied) Fit 2

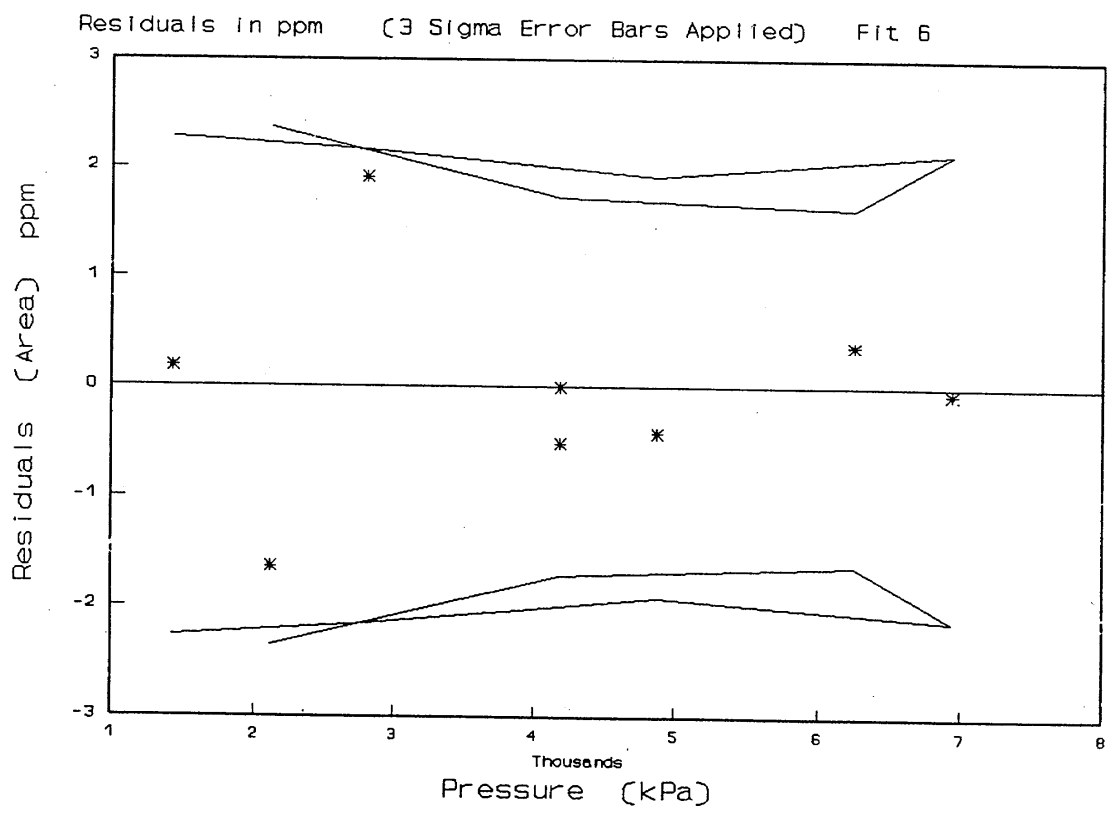
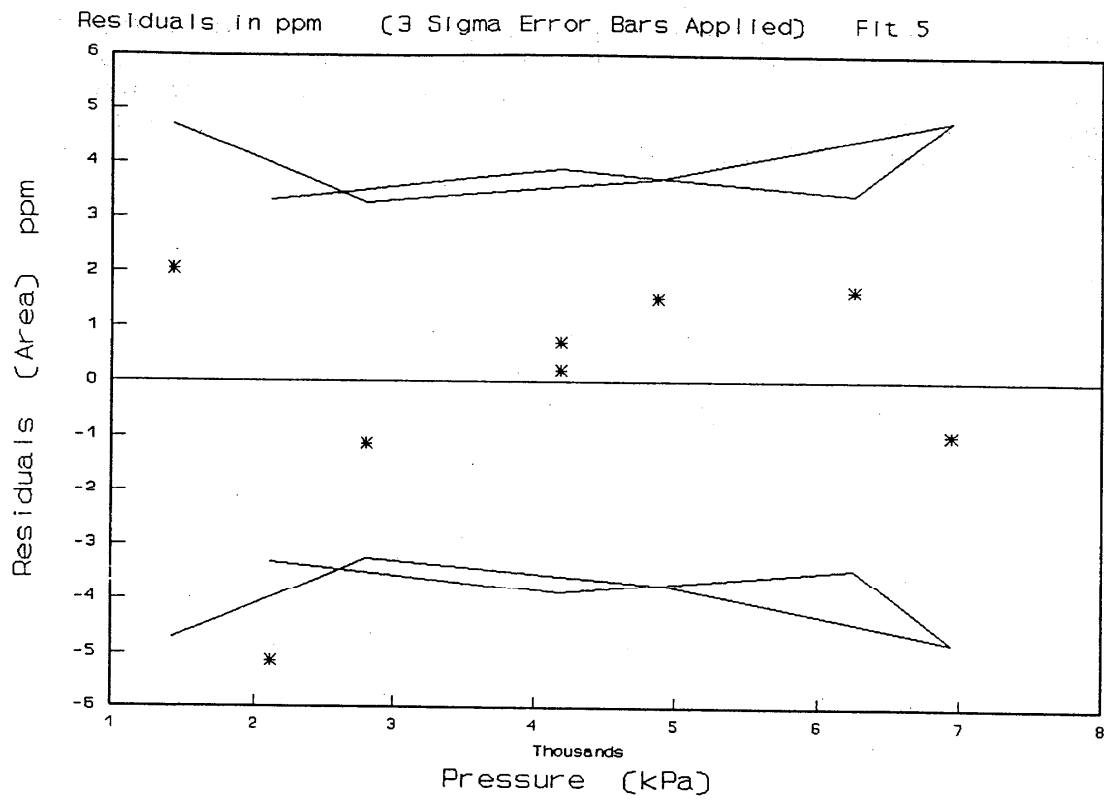


Residuals in ppm (3 Sigma Error Bars Applied) Fit 3



Residuals in ppm (3 Sigma Error Bars Applied) Fit 4





The results of the test, as determined by using the AREA EQUATIONS, are compiled in this table. It lists the coefficients and their tripled standard deviations due to random sources of errors and, for the highest pressure, the uncertainty in pressure due to the uncertainty in these coefficients.

COEFF, FIT 1	COEFF, FIT 2	COEFF, FIT 3	COEFF, FIT 4	
1.422472E-04	1.422463E-04	1.422481E-04	1.422441E-04	AREA, m ²
0.000000E+00	0.000000E+00	-1.481821E-12	2.194630E-12	PRES COEF b ₁ Pa ⁻¹
0.000000E+00	0.000000E+00	0.000000E+00	0.000000E+00	PRES COEF b ₂ Pa ⁻²
0.000000E+00	0.000000E+00	0.000000E+00	0.000000E+00	
0.000000E+00	-2.819330E-03	0.000000E+00	-5.631232E-03	TARE, N
4.614187E-06	4.344092E-06	8.381819E-06	1.168489E-05	3 STD DEV A ₀ /A ₀₋₁
0.000000E+00	0.000000E+00	1.826769E-12	1.597867E-12	3 STD DEV b ₁ Pa ⁻¹
0.000000E+00	0.000000E+00	0.000000E+00	0.000000E+00	3 STD DEV b ₂ Pa ⁻²
0.000000E+00	0.000000E+00	0.000000E+00	0.000000E+00	
0.000000E+00	1.566954E-03	0.000000E+00	2.238437E-03	3 STD DEV T, N
1.459134E-05	7.183315E-06	1.173177E-05	4.149265E-06	3 RES STD DEV A/A
4.614187E-06	5.931598E-06	2.105778E-05	2.504029E-05	3 STD DEV A _e /A _e at P _{max}
COEFF, FIT 5	COEFF, FIT 6	COEFF, FIT 7	COEFF, FIT 8	
1.422498E-04	1.422401E-04	1.422477E-04	1.422452E-04	AREA, m ²
-8.910301E-12	1.058918E-11	0.000000E+00	0.000000E+00	PRES COEF b ₁ Pa ⁻¹
8.864457E-19	-7.183443E-19	-1.411765E-19	1.757731E-19	PRES COEF b ₂ Pa ⁻²
0.000000E+00	0.000000E+00	0.000000E+00	0.000000E+00	
0.000000E+00	-9.268421E-03	0.000000E+00	-4.561128E-03	TARE, N
1.133755E-05	3.704057E-05	6.535885E-06	7.376934E-06	3 STD DEV A ₀ /A ₀₋₁
6.351027E-12	1.083068E-11	0.000000E+00	0.000000E+00	3 STD DEV b ₁ Pa ⁻¹
7.450572E-19	9.206452E-19	2.397935E-19	1.531932E-19	3 STD DEV b ₂ Pa ⁻²
0.000000E+00	0.000000E+00	0.000000E+00	0.000000E+00	
0.000000E+00	4.978454E-03	0.000000E+00	1.829370E-03	3 STD DEV T, N
7.468447E-06	3.240224E-06	1.312718E-05	4.679866E-06	3 RES STD DEV A/A
9.128167E-05	1.615673E-04	1.808189E-05	1.660652E-05	3 STD DEV A _e /A _e at P _{max}

Run 01/04/94 11:09:22.45

As shown in the Residual Plots in ppm on the preceding pages the Maximum uncertainty values in ppm for Fits 1 - 6 are:

1	2	3	4	5	6
9.1	4.7	6.4	3.0	5.1	2.4